

DIGITAL SIMULATION OF TRANSIENTS OF THE
STEAM GENERATOR OF PRESSURIZED
WATER NUCLEAR REACTOR

By

ARAVINDA KAR

Th
NETP/1980/m
K144d



NUCLEAR ENGINEERING TECHNOLOGY PROGRAMME
INDIAN INSTITUTE OF TECHNOLOGY, KANPUR
JULY, 1980

DIGITAL SIMULATION OF TRANSIENTS OF THE STEAM GENERATOR OF PRESSURIZED WATER NUCLEAR REACTOR

A Thesis Submitted
In Partial Fulfilment of the Requirements
for the Degree of
MASTER OF TECHNOLOGY

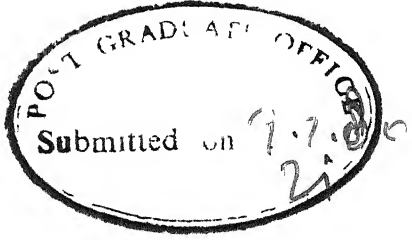
By
ARAVINDA KAR

to the
NUCLEAR ENGINEERING TECHNOLOGY PROGRAMME
INDIAN INSTITUTE OF TECHNOLOGY, KANPUR
JULY, 1980

I.I.T. KANPUR
CENTRAL LIBRARY
Acc. No. A 63023

- 8 AUG 1980

NETP - 1980 - M - KAR - DIG



CERTIFICATE

This is to certify that this work on "Digital Simulation of Transients of the Steam Generator of Pressurized Water Nuclear Reactor" has been carried out under my supervision and it has not been submitted elsewhere for a degree.

K. Sri Ram

Head,
Nuclear Engineering and Technology
Programme,
Indian Institute of Technology, Kanpur.

ACKNOWLEDGEMENTS

It gives me a great pleasure to express my indebtedness and profound regard to my teacher, Professor K. Sri Ram for his valuable suggestions and continuous encouragement at each stage of this work. I am especially grateful for the opportunity of becoming acquainted with his methods of approach to scientific problems.

I gratefully acknowledge the typing skill of Mr. J.P. Gupta and meticulous cyclostyling of Mr. Tripathi.

(A. Kar)

CONTENTS

Page No.

CERTIFICATE

ACKNOWLEDGEMENTS

LIST OF FIGURES

NOMENCLATURE

ABSTRACT

Chapter 1 - INTRODUCTION

1.1	Introduction	1
1.2	Review of Dynamic Models for Steam Generators	2
1.3	Present Work	3

Chapter 2 - THE STEAM GENERATOR

2.1	A brief description of the steam generator	5
2.2	Model of the steam generator	7

Chapter 3 - ANALYTICAL MODEL FOR SIMULATING THE STEAM GENERATOR

3.1	Model for the steady state	10
3.1.1	Fundamental equations of conservation	10
3.1.2	Equations of conservation at steady state	11
3.1.3	Equation of conservation of energy	11
3.1.4	Equation of conservation of momentum	12

Page No.

3.1.5	Flow patterns and heat transfer	13
3.2	Mathematical model for simulating the transients	14
3.2.1	Equations for analysing the transients	14
3.2.2	Equation of conservation of energy	16
3.2.3	System of equations	17
3.2.4	Solution of the system of equations	24

Chapter 4 - DESCRIPTION OF THE COMPUTER CODE

4.1	Input variables	31
4.2	Steady state calculation	36
4.2.1	Flow chart	37
4.2.2	Subroutines	37
4.3	Transient calculation	44
4.3.1	Flow chart	44
4.3.2	Subroutines	44

Chapter 5 - RESULTS AND DISCUSSIONS

5.1	Results and discussions	54
5.1.1	Steady state values	54
5.1.2	Transient values	54
5.2	Conclusions	56
	References	82
	Appendix A	84

	<u>Page No.</u>
Appendix B	86
Appendix C	88
Sample data	91
Programme Listing	94

NOMENCLATURE

A	-	Cross sectional area for flow, ft ²
A _T	-	Heat transfer area, ft ²
C _P	-	Specific heat at constant pressure, Btu/lbm
D _e	-	Equivalent diameter, ft
\bar{d}	-	Spacing of the tubes, inch.
d _e	-	External diameter of the tubes of primary circuit, inch.
d _i	-	Internal diameter of the tubes of primary circuit, inch.
e	-	Energy per unit mass, Btu/lbm
F _K	-	Frictional force, lbf
f	-	Friction coefficient
G	-	Mass flux, lbm/ft ² -hr
g	-	Acceleration due to gravity, ft/sec ²
ξ_c	-	Conversion ratio, lbm-ft/lbf-sec ²
H	-	Specific enthalpy, Btu/lbm
H _{fg}	-	Latent heat of vaporazition, Btu/lbm
H _{in}	-	Enthalpy at the inlet of the generator, Btu/lbm
h	-	Heat transfer coefficient, Btu/hr-ft ² -°F
J	-	Mechanical equivalent of heat, J = 778 lbf-ft/Btu
k	-	Thermal Conductivity, Btu/hr-ft-°F

- L_{ev} - Length of the evaporator, ft
- L_{PA} - Length of the preheater, ft
- P_m - Wetted perimeter, ft
- P - Pressure, Psi
- ΔP - Pressure drop, Psi
- Q - Rate of heat transfer, Btu/hr
- \dot{q} - Heat flux, Btu/hr-ft²
- T - Temperature, °F
- T_p - Temperature of the wall of the tube, °F
- ΔT_{sat} - $T_p - T_{Sat}$, °F
- u - Internal energy, Btu/lbm
- U - Total internal energy, Btu/lbm
- v - Velocity, ft/hr
- v - Specific volume, ft³/lbm
- w - Mass flow rate, lbm/hr
- x, z - Quality of vapour
- X_{tt} - Lockhart and Martinelli's parameter
- Z - Direction of flow
- ΔZ - Height of each control volume, ft.

Greek Letters:

- α - Void fraction.
- μ - Viscosity, lbf/hr-ft
- ρ - Density, lbm/ft³
- σ - Surface tension, lbf/ft
- β_{LO}^2 - Multiplicator for calculating frictional pressure drop in two-phase flow.
- γ - Empirical constant used in Thom's correlation for calculating the void-fraction.

Superscript:

- Refers to the value at the middle of a control volume.

Subscript:

- e - Refers to the exit
- ev - Evaporator
- f - Saturated liquid condition
- s - Saturated vapour condition
- i - Inlet condition
- iso - Refers to isothermal condition
- j - Refers to junction
- l - Saturated liquid.

P - Refers to primary circuit
PA - Refers to preheater
S - Refers to secondary circuit
Sat - Saturation condition
v - Saturated vapour condition
c.v. - Control volume

Dimensionless Groups:

Nu - Nusselt No. = $h \cdot D_e / k$
Pr - Prandtl No. = $\mu \cdot C_p / k$
Re - Reynolds No. = $G \cdot D / \mu$.

LIST OF FIGURES

	<u>Page No.</u>		
Fig. 2.1	-	A schematic of an integral economizer U-tube steam generator (IEUTSG)	6
Fig. 2.2	-	Simulation model of the steam generator	8
Fig. 4.1	-	Flow chart of the computer programme calculating the steady state values	49
Fig. 4.2	-	Flow chart of the programme simulating the transients	50
Fig. 4.3	-	Flow chart of the subroutine SOLUC	52
		Effect of perturbation in the mass flow rate of the primary circuit on	
Fig. 5.1a	-	Pressure	58
Fig. 5.1b	-	Temperature	59
Fig. 5.1c	-	Mass flow rate	60
Fig. 5.1d	-	Quality at the exit of the evaporator	61
		Effect of perturbation in the pressure of the primary circuit on	
Fig. 5.2a	-	Pressure	62
Fig. 5.2b	-	Temperature	63
Fig. 5.2c	-	Mass flow rate	64
Fig. 5.2d	-	Quality at the exit of the evaporator	65
		Effect of perturbation in the internal energy of the liquid in the primary cir- cuit on	

Fig. 5.3a	-	Pressure	66
Fig. 5.3b	-	Temperature	67
Fig. 5.3c	-	Mass flow rate	68
Fig. 5.3d	-	Quality at the exit of the evaporator	69
Effect of perturbation in the mass flow rate of the secondary circuit on			
Fig. 5.4a	-	Pressure	70
Fig. 5.4b	-	Temperature	71
Fig. 5.4c	-	Mass flow rate	72
Fig. 5.4d	-	Quality at the exit of the evaporator	73
Effect of perturbation in the pressure of the secondary circuit on			
Fig. 5.5a	-	Pressure	74
Fig. 5.5b	-	Temperature	75
Fig. 5.5c	-	Mass flow rate	76
Fig. 5.5d	-	Quality at the exit of the evaporator	77
Effect of perturbation in the internal energy of the feed water in the secondary circuit on			
Fig. 5.6a	-	Pressure	78

Page No.

Fig. 5.6b	- Temperature	79
Fig. 5.6c	- Mass flow rate	80
Fig. 5.6d	- Quality at the exit of the evaporator	81

ABSTRACT

A digital computer code was developed to simulate the transient behaviour of a steam generator typically used in pressurized water reactor nuclear power plants.

The three fundamental equations of conservation of mass, energy and momentum were converted to a set of linear algebraic equations using finite difference method, from which an explicit numerical scheme was formulated.

On the primary side single phase flow and forced convection heat transfer were assumed and on the secondary side the possibility of the existence of different flow regimes was assumed and the heat transfer in these regimes was calculated using appropriate correlations.

CHAPTER 1

INTRODUCTION

1.1 Introduction:

With the present interest in the safety studies of nuclear reactor behaviour, it becomes important to study the behaviour of various reactor components. Steam generator forms an integral part of the nuclear power plants where heat is exchanged between the primary coolant, which flows through the core of the nuclear reactor, and the secondary fluid, which provides power for the turbine. The steam generator presents complexity in modeling because, even under normal conditions both subcooled and boiling heat transfer occur on the secondary side.

Modeling of a large system via state variable methods is quite difficult because of the fact that the overall system has to be broken down into separate models for each of the sub-systems and then these sub-system models have to be coupled to construct the overall system model.

Dynamic modeling plays an important role particularly in nuclear power plants because of stringent safety requirements to ensure failsafe operation of the plant. Though a great deal of care is taken to ensure public safety in nuclear power plants there is always a finite probability that a system may fail and lead to an undesirable situation. Transient analysis allows us

to study the degree of danger one may encounter due to the failure of an equipment under a disturbed condition and it gives guidelines for proper instrumentation to prevent such accidents. In case of a steam generator a large number of possibilities which may perturb its steady operation can be enumerated. The steam generator has primary and secondary circuit. In the primary circuit there may be reduced flow rate of liquid due to loss of coolant accident (LOCA) which generally occurs due to the rupture in the pipe, discharge from the high-pressure system to a low-pressure system. There may also be loss of flow accidents (LOFA) due to the improper opening of valves and pump failure. This disturbance in coolant flow in turn affects the pressure and the temperature of the liquid in the primary heat transport system. Similarly the change in the feed water flow in the secondary circuit will alter the steam output and this may upset the operation of the turbines which will affect the power output of the whole power station. So transient analysis of the steam generator is essential to ensure that it can accommodate a certain amount of perturbation and does not fail to complicate the situation if there is an accident.

1.2 Review of Dynamic Models for Steam Generators:

In the literature there are no simplified models available for simulating the steam generators excepting the complicated

models of the reactor thermal hydraulic computer codes such as RELAP-4 [1] and FLASH [2] etc.

Recently a mathematical model was developed by Arwood and Kerlin [3] to simulate the U-tube steam generator. This paper uses linearized equations to predict the behaviour around a steady state operating point. The detailed heat transfer regimes are not considered explicitly.

Hoeld [4] developed a nonlinear transient model for the calculation of the dynamic behaviour of a vertical natural-circulation U-tube steam generator (UTSG). But modern nuclear power plants use IEUTSG which is an improved version of UTSG and has higher heat transfer effectiveness.

I.M.D. Silva [5] developed a model for simulating the transients of an IEUTSG. This model takes various flow regimes and different heat transfer regimes into account and follows an implicit numerical technique for calculating the dynamic behaviour of the steam generator.

1.3 Present Work:

The present work consists of developing a model to simulate the transient behaviour of an integral economizer U-tube steam generator (IEUTSG) utilized in a 600 MW_e PWR. To give an accurate representation of the steam generator, due considerations have been given to the aspects of two-phase flow and heat transfer.

As fundamental equations the well-known conservation equations for mass, energy and momentum have been chosen. Additional approximation equations for the thermo dynamic properties of water and steam, for a two-phase correlation, for one and two-phase friction coefficients and for the heat conduction coefficients have been established.

For steady state (starting) values the model and computer code developed by Armando Costa Pinto [6] has been used.

CHAPTER 2

THE STEAM GENERATOR

2.1 A brief description of the steam generator [7]:

A schematic of the steam generator is given in figure 2.1. Various components that constitute the steam generator are:

(a) Primary Side:

The hot primary fluid coming from the nuclear reactor enters the steam generator at the primary inlet plenum. The fluid then enters the upward portion (hot leg) of the U-tubes. The primary flow continues into the downward side (cold leg) and into the economizer section.

(b) Tube Metal Walls:

The tube metal walls separate the primary and the secondary fluids. Heat is transferred from the primary to the secondary fluid through the tube walls at a rate determined by the overall heat transfer coefficient and the temperature difference.

(c) Secondary Side:

In this side there is an economizer just above the bottom plenum. This economizer is nothing but a closed container which covers a portion of the cold legs and separates them from the rest of the secondary side. The

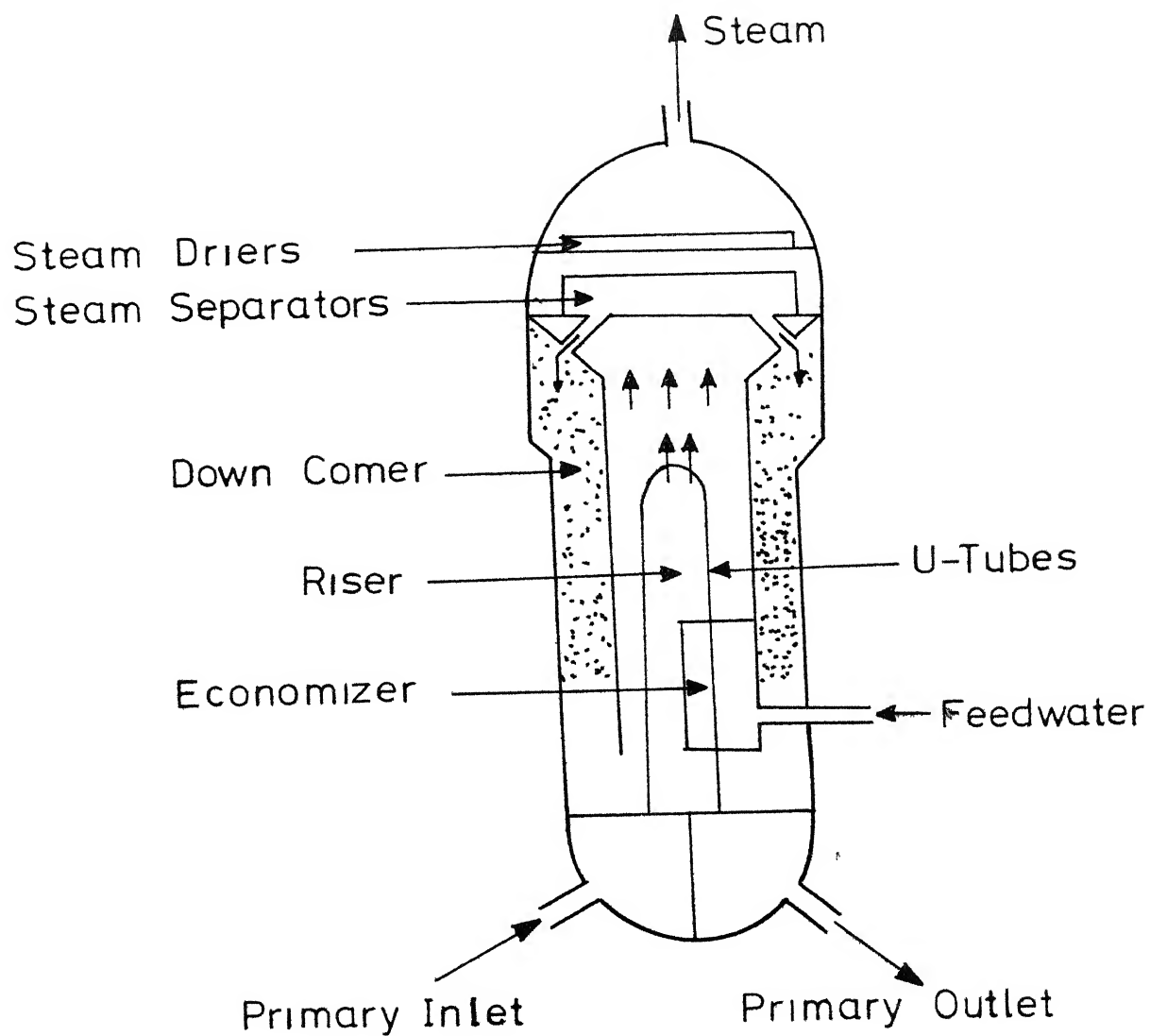


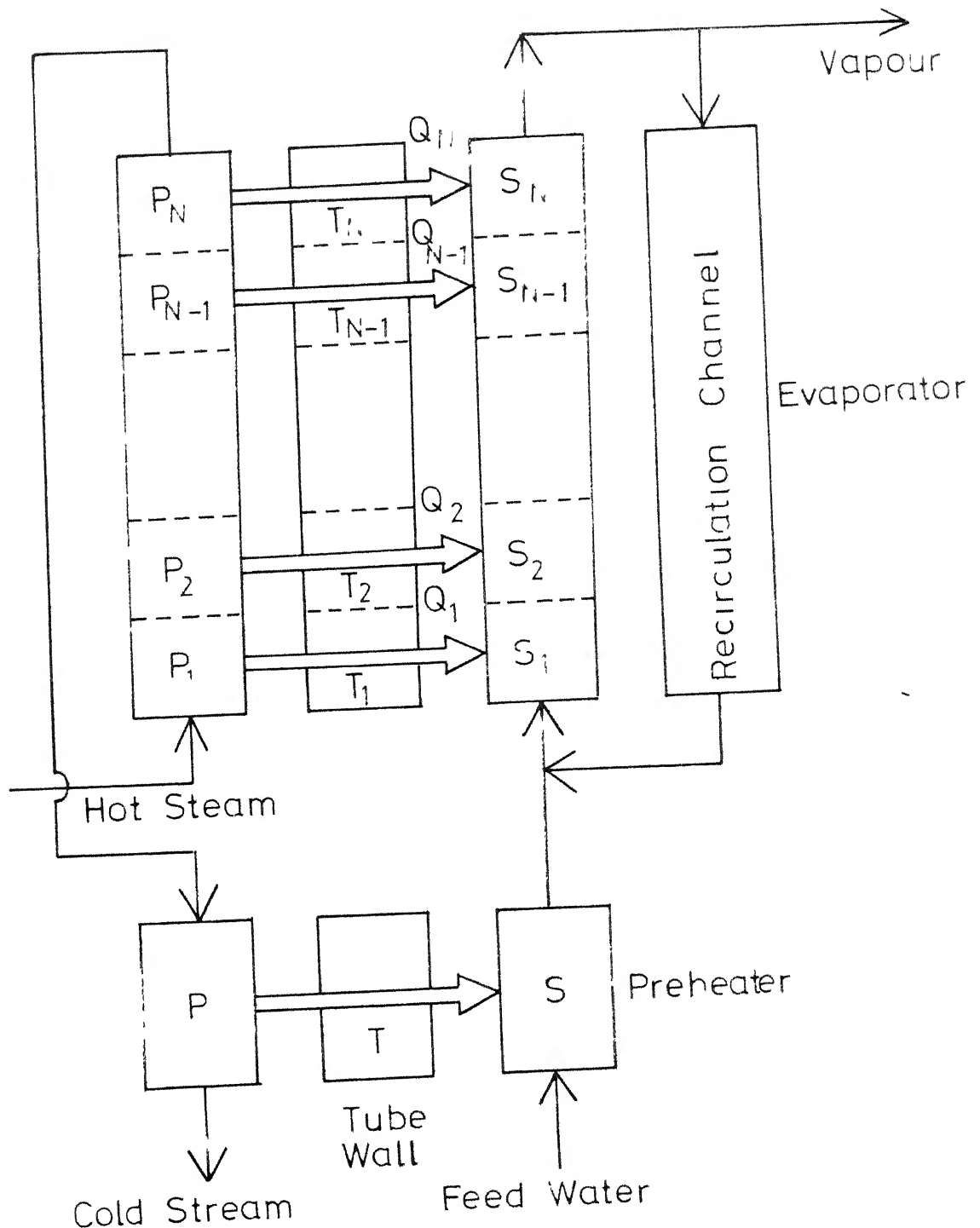
Fig. 2.1 A schematic of an Integral Economizer U-Tube Steam Generator (IEUTSG)

feedwater enters the evaporator through this economizer.

The IEUTSG design is a modification of the recirculation type U-tube steam generator (UTSG) used in many operating PWR's. The design change has been made to increase the heat transfer effectiveness of the system. The standard UTSG design is similar to that of the IEUTSG, but all of the feedwater is introduced into the downcomer and there is no economizer section. Because of the high recirculation ratio, the water entering the heated section from the downcomer is near the saturation temperature. As a result, there is a small temperature difference between the primary water of the cold legs and the secondary water in a UTSG. The purpose of the introduction of colder feedwater directly into this region in the IEUTSG design is to increase the temperature difference and increase the heat transfer from the primary water.

2.2 Model of the steam generator [6]:

The steam generator model used in the present study is shown in Fig. 2.2. The steam generator is represented in two sections, preheater (economizer) and an evaporator. In reality the steam generators of the PWR's have U-tube geometry, the present model simplifies it to parallel tube geometry but retains all the significant factors such as the total heat transfer area, total amount of heat transferred, preheater. Lack of detailed data about the internals of the steam generator, such



→ Indicate heat transfer
 P — Primary Circuit S — Secondary Circuit
 T — Temperature of tube Q — Heat Flux

Fig. 2.2 Simulation model of Steam Generator

as the pressure drop due to baffles, quality of steam at the outlet of the generator before the steam separator etc. is circumvented by the pressure balance and heat balance equations as described in the later chapters.

As indicated in the figure the coolant from the reactor outlet enters the primary side of the generator as a hot stream in the evaporator section and leaves the generator from the preheater section as a cold stream to enter the reactor. The heat flow from the primary side is conducted through the tube walls of the steam generator and enters the secondary stream. The figure also indicates that the secondary stream leaves the evaporator section of the generator as vapor and part of the stream is recirculated. Some make up feedwater enters the preheater section and mixes with the secondary stream after the preheater.

CHAPTER 3

Analytical Model for Simulating the Steam Generator

3.1 Model for the steady state:

A simplified mathematical model and a computer code were developed by A.C. Pinto [7] for the steady state analysis of a steam generator utilized in a 600 MWe pressurized water reactor nuclear power plants. This model takes different flow patterns and the corresponding heat transfer regimes into account. The details of this model can be found in reference 6. However, a brief description of this model is given in the following sections.

3.1.1 Fundamental equations of conservation:

In the steady state model [7] it is assumed that the flow is vertical. There is no transfer of work across each control volume indicated in Fig. 2.2. The area of flow cross section is assumed constant. Thus the three fundamental equations of mass, energy and momentum conservation become

$$\text{Mass} \quad A \frac{\partial \rho}{\partial t} = - \frac{\partial W}{\partial Z} \quad (3.1)$$

where $W = \rho AV$.

$$\text{Energy:} \quad A \frac{\partial}{\partial t} (\rho_e) = \dot{q} \frac{\partial A_T}{\partial Z} - \frac{\partial (We)}{\partial Z} - \frac{\partial (PAV)}{\partial Z} \quad (3.2)$$

where $e = u + \frac{V^2}{2} + gZ$ is the energy per unit mass of the fluid.

$$\text{Momentum: } A \cdot \frac{\partial (\rho V)}{\partial t} = - A \frac{\partial P}{\partial Z} - \frac{\partial F_K}{\partial Z} - \rho g - \frac{\partial (WV)}{\partial Z} \quad (3.3)$$

3.1.2 Equations of conservation at steady state:

At steady state the rate of change of any property with respect to time is zero. So the equations 3.1, 3.2 and 3.3 will become

$$W = \text{Constant} \quad (3.4)$$

$$\ddot{A} \frac{dA_T}{dz} - \frac{d(W_e)}{dz} - \frac{d}{dz} (PAV) = 0 \quad (3.5)$$

$$- A \frac{dP}{dz} - \frac{dF_K}{dz} - \frac{d(WV)}{dz} - A \rho g = 0 \quad (3.6)$$

3.1.3 Equation of conservation of energy [7]:

Using the relations

$$e = u + \frac{V^2}{2} + gZ$$

$$H = u + \frac{P}{\rho}$$

$$W = \rho AV$$

$$G = W/A$$

$$v = 1/\rho$$

the equation 3.5 can be transformed to the following form
(for details see appendix A):

$$\ddot{q} \frac{dA_T}{dz} - W \frac{dH}{dz} - WG^2 v \frac{dv}{dz} - Wg = 0 \quad (3.7)$$

Integrating this equation with respect to Z from junction n to $n+1$, the limits of control volume n, we get

$$H_{n+1} = H_n + \bar{Q}_n - \frac{G^2}{2 \cdot g_c \cdot J} (v_{n+1}^2 - v_n^2) - \frac{g}{g_c} \cdot \frac{1}{J} \cdot \Delta Z \quad (3.8)$$

where $\bar{Q}_n = \int \ddot{q} dA_T = \ddot{q}_n \cdot A_T$ is the total amount of
Control volume n

heat transfer in control volume n.

3.1.4 Equation of conservation of momentum [7]:

Let us integrate the equation 3.6 with respect to Z from the centre of control volume ($n-1$) to that of control volume n. The following two assumptions are made to simplify the integration.

- (a) The frictional pressure in one half of any control volume is equal to one half of the frictional pressure of the whole control volume.
- (b) The velocity of fluid at the outlet of control volume ($n-1$) is equal to the velocity of the fluid at the inlet of control volume n.

Utilizing these two assumptions and the relationship $G = W/A$, we get (for details see appendix B) the following equation.

$$\bar{P}_n = \bar{P}_{n-1} - \frac{1}{2 \cdot A} (\bar{F}_{K,n-1} + \bar{F}_{K,n}) - \frac{G}{144 \cdot g_c} (v_n - \bar{v}_{n-1}) \\ - \frac{G}{144 \cdot g_c} (\bar{v}_n - v_n) - \frac{g}{144 \cdot g_c} \cdot \frac{\Delta Z}{v_n} \quad (3.9)$$

The quantity without bar represents the value at the junction and the quantity with bar represents the average value in a control volume.

An examination of the terms of equation 3.9 will lead it to the following familiar form.

$$\bar{P}_n = \bar{P}_{n-1} + \frac{1}{2} [(\Delta P_{frictional})_{C.V.(n-1)} + (\Delta P_{frictional})_{C.V.(n)}] \\ - (\Delta P_{acceleration})_{C.V.(n-1) j.n} - (\Delta P_{acceleration})_{j.n C.V(n)} \\ - (\Delta P_{elevation}) \quad (3.10)$$

3.1.5 Flow patterns and heat transfer [6]:

The liquid in the primary heat transport system of the steam generator is always in the form of compressed liquid and hence the mode of heat transfer is pure convection. On the secondary side the liquid enters the generator as saturated

liquid. The secondary liquid will encounter bubbly flow and annular flow regimes and the heat transfer regimes will be pure convection, local boiling, nucleate boiling, forced convection and stable film boiling. The various flow regimes and the heat transfer modes and the correlations used in each mode are indicated in Table 3.1

3.2 Mathematical Model for Simulating the Transients

The model developed to simulate the transients of the steam generator has been described in details in the following sections.

3.2.1 Equations of conservation for analysing the transients:

The conservation equations are:

$$\text{Mass: } A \frac{\partial \rho}{\partial t} = - \frac{\partial W}{\partial Z} \quad (3.11)$$

$$\text{Energy: } A \frac{\partial (\rho e)}{\partial t} = \dot{q} \frac{\partial A_T}{\partial Z} - \frac{\partial (We)}{\partial Z} - \frac{\partial (PAV)}{\partial Z} \quad (3.12)$$

$$\text{Momentum: } A \frac{\partial (\rho V)}{\partial t} = -A \frac{\partial P}{\partial Z} - \frac{\partial F_K}{\partial Z} - A \rho g - \frac{\partial (WV)}{\partial Z} \quad (3.13)$$

where $e = u + V^2/2 + gZ$ is the energy per unit mass of the fluid. It can be assumed that the effect of g is negligibly small and hence the term gZ in the expression of e and $A \rho g$ of equation 3.13 can be neglected.

Mode	Flow Regime	Heat Transfer Regime	Heat Transfer Correlation
1	Single phase compressed liquid	Pure convection	Dittus Boelter equation [9]: $N_u = 0.023 Re^{0.8} Pr^{0.4}$
2	Single phase compressed liquid	Local boiling	Thom's correlation [9]
3	Bubbly flow	Nucleate boiling	$T_p - T_{Sat} = \frac{0.072 (\dot{q})^{1/2}}{\text{Exp}(P/1260)}$
4	Annular flow	Evaporation by forced convection	Chen's correlation [8]: $h = S(0.00122)A + F(0.023)Re_1^{0.8} Pr_1^{0.4} \cdot \frac{k_1}{D_e}$ $A = \frac{k_1^{0.79} c_1^{0.45} \rho_1^{0.49} \epsilon_c^{0.25} \Delta T^{0.24}}{\sigma^{0.5} \mu_1^{0.29} H_{fg} \alpha_v^{0.20}}$
5	Annular flow	Stable film boiling	F and S are obtained using the polynomials given in chapter 5. Polomik's correlation [9]: $\frac{h D_e}{k_{film}} = 0.0136 (Re_{film} \frac{1-x}{x})^{0.853} \frac{\alpha}{1-\alpha} Pr_{film}$

Table 3.1

3.2.2 Equation of conservation of energy:

Using $e = u + V^2/2$ the equation 3.12 can be written as

$$A \frac{\partial(\rho u + \rho V^2/2)}{\partial t} = \dot{q} \frac{\partial A_T}{\partial Z} - \frac{\partial(Wu + WV^2/2)}{\partial Z} - \frac{\partial(PAV)}{\partial Z}$$

which on simplification yields

$$\begin{aligned} A \frac{\partial(\rho u)}{\partial t} + A\rho V \frac{\partial V}{\partial t} + \frac{AV^2}{2} \frac{\partial \rho}{\partial t} &= \dot{q} \frac{\partial A_T}{\partial Z} - \frac{\partial(Wu)}{\partial Z} - WV \frac{\partial V}{\partial Z} \\ &- \frac{V^2}{2} \cdot \frac{\partial W}{\partial Z} - \frac{\partial}{\partial Z}(PAV) \end{aligned}$$

Substituting in this equation the value of $A \frac{\partial \rho}{\partial t}$ we get on simplification

$$A \frac{\partial(\rho u)}{\partial t} = \dot{q} \frac{\partial A_T}{\partial Z} - A\rho V \frac{\partial V}{\partial t} - \frac{\partial(Wu)}{\partial Z} - \frac{\partial(PAV)}{\partial Z} - WV \frac{\partial V}{\partial Z} \quad (3.12a)$$

From equation 3.13 we get

$$A\rho \frac{\partial V}{\partial t} + AV \frac{\partial \rho}{\partial t} = - A \frac{\partial P}{\partial Z} - W \frac{\partial V}{\partial Z} - V \frac{\partial W}{\partial Z} - \frac{\partial F_K}{\partial Z}$$

Multiplying both sides by V and substituting the value of $A \frac{\partial \rho}{\partial t}$ into this equation we get on simplification

$$A\rho V \frac{\partial V}{\partial t} = -AV \frac{\partial P}{\partial Z} - WV \frac{\partial V}{\partial Z} - V \frac{\partial F_K}{\partial Z} \quad (3.13a)$$

Substituting the value at $A\rho V \frac{\partial V}{\partial t}$ in the equation 3.12a it can be simplified to the following form.

$$A \frac{\partial(\rho u)}{\partial t} = \ddot{q} \frac{\partial A_T}{\partial Z} - \frac{\partial(Wu)}{\partial Z} - PA \frac{\partial V}{\partial Z} + V \frac{\partial F_K}{\partial Z} \quad (3.12b)$$

3.2.3 System of equations:

We now have the following system of equations to be used to simulate the transients.

$$A \frac{\partial(\rho V)}{\partial t} = -A \frac{\partial P}{\partial Z} - \frac{\partial(WV)}{\partial Z} - \frac{\partial F_K}{\partial Z} \quad (3.14)$$

$$A \frac{\partial(\rho u)}{\partial t} = \ddot{q} \frac{\partial A_T}{\partial Z} - \frac{\partial(Wu)}{\partial Z} - PA \frac{\partial V}{\partial Z} + V \frac{\partial F_K}{\partial Z} \quad (3.15)$$

$$A \frac{\partial p}{\partial t} = - \frac{\partial W}{\partial Z} \quad (3.16)$$

Integration of these equations with respect to Z over a control volume i bounded by junction i and $i+1$ will lead to the following forms.

(a) The equation of momentum conservation gives:

$$\frac{\partial}{\partial t} \int_i^{i+1} A \rho V \, dz = - \int_i^{i+1} \frac{\partial(WV)}{\partial Z} \, dz - \int_i^{i+1} \frac{\partial F_K}{\partial Z} \, dz - A \int_i^{i+1} \frac{\partial P}{\partial Z} \, dz$$

$$\text{Let us define } \bar{W}_i = \frac{\int_i^{i+1} A \rho V \, dz}{\int_i^{i+1} dz}$$

With this definition we get

$$\frac{d\bar{W}_i}{dt} = -A(\bar{P}_{i+1} - \bar{P}_i) - [WV|_{i+1} - WV|_i] - \bar{F}_{Ki}$$

But $W = \rho AV$, i.e., $WV = W^2/\rho A$ and

$$\bar{F}_{Ki} = \bar{f}_i \frac{\frac{W_i^2}{\rho_i}}{2AD_e} \Delta Z$$

So the momentum equation takes the form:

$$\bar{W}_i = \frac{A}{\Delta Z} (\bar{P}_i - \bar{P}_{i+1}) + \frac{1}{A \cdot \Delta Z} \left(\frac{W_i^2}{\rho_i} - \frac{W_{i+1}^2}{\rho_{i+1}} \right) - \bar{f}_i \frac{\frac{W_i^2}{\rho_i}}{2AD_e}$$

(3.17)

(b) The equation of energy conservation will give:

$$\begin{aligned} \frac{\partial}{\partial t} \int\limits_i^{i+1} A\rho u \, dZ &= \int\limits_i^{i+1} \bar{q} \frac{\partial A_T}{\partial Z} \, dZ - \int\limits_i^{i+1} \frac{\partial (wu)}{\partial Z} \, dZ \\ &\quad - \int\limits_i^{i+1} PA \frac{\partial V}{\partial Z} \, dZ + \int\limits_i^{i+1} V \frac{\partial F_K}{\partial Z} \, dZ \end{aligned}$$

We now define

$$\begin{aligned} \bar{U}_i &= \int\limits_i^{i+1} A\rho u \, dZ \\ \bar{Q}_i &= \int\limits_i^{i+1} \bar{q} \frac{\partial A_T}{\partial Z} \, dZ \end{aligned}$$

$$\int\limits_i^{i+1} P_A \frac{\partial V}{\partial Z} dZ - \bar{P}_i A (V_{i+1} - V_i) = P_i \left(\frac{W_{i+1}}{\rho_{i+1}} - \frac{W_i}{\rho_i} \right)$$

and

$$\int\limits_i^{i+1} V \frac{\partial F_K}{\partial Z} dZ = \bar{V}_i \bar{F}_{K,i} = \bar{f}_i \frac{\frac{\partial W_i}{\partial Z}}{2A^2 D_e \bar{\rho}_i^2} \cdot \Delta Z$$

With these simplifying assumptions we get

$$\begin{aligned} \dot{\bar{U}} &= \bar{Q}_i + W_i u_i - W_{i+1} u_{i+1} - \int\limits_i^{i+1} \left(\frac{W_{i+1}}{\rho_{i+1}} - \frac{W_i}{\rho_i} \right) \\ &\quad + \bar{f}_i \frac{\frac{\partial W_i}{\partial Z}}{2A^2 D_e \bar{\rho}_i^2} \cdot \Delta Z \end{aligned} \quad (3.18)$$

(c) The equation of mass conservation gives:

$$\frac{\partial}{\partial t} \int\limits_i^{i+1} A \rho dz = - \int\limits_i^{i+1} \frac{\partial W}{\partial Z} dz$$

Let us define $\bar{\rho}_i$

$$\bar{\rho}_i = \frac{\int\limits_i^{i+1} A \rho dz}{\int\limits_i^{i+1} A dz}$$

With this definition we get

$$\frac{\dot{\bar{\rho}}_i}{\bar{\rho}_i} = \frac{1}{A \cdot \Delta Z} (W_i - W_{i+1}) \quad (3.19)$$

Equations 3.17, 3.18 and 3.19 have to be modified to incorporate the two-phase multiplier r and make the units consistent. To make the units consistent we have to multiply appropriate term by any one of the following three factors.

$$C_1 = g_c \times 3600^2 \frac{\text{sec}^2}{\text{Hr}^2} \times 144 \frac{\text{in}^2}{\text{ft}^2} = 0.600444 \times 10^{11}$$

$$c_2 = 144 \frac{\text{in}^2}{\text{ft}^2} \times 0.001285 \frac{\text{Btu}}{\text{lbf-ft}} = 0.18504$$

$$c_3 = \frac{1}{g_c} \times \frac{Hr^2}{3600^2 \text{ Sec}^2} \times 0.001285 \frac{\text{Btu}}{\text{lbf-ft}} = 0.308172 \times 10^{-11}$$

Now we have

$$\frac{\Delta p}{\Delta z} = \frac{1}{A \cdot \Delta Z} (w_i - w_{i+1}) \quad (3.20)$$

$$\dot{\overline{U}}_i = \overline{Q}_1 + w_i u_i - w_{i+1} u_{i+1} - \overline{I}_i c_2 \left(\frac{w_{i+1}}{p_{i+1}} - \frac{w_i}{p_i} \right)$$

$$+ c_3 \frac{\bar{f}_i \bar{w}_i^3 \Delta z}{2A^2 D_e \bar{\rho}_i^2} \quad (3.21)$$

$$\frac{\dot{w}_i}{w_i} = \frac{c_1 A}{\Delta Z} \left(\frac{p_i}{r_i} - \frac{p_{i+1}}{r_{i+1}} \right) - \frac{\bar{x}_i \bar{w}_i^2}{2A D_e \bar{p}_i} + \frac{1}{A \cdot \Delta Z} \left(\frac{r_i w_i^2}{p_i} - r_{i+1} \frac{w_{i+1}^2}{p_{i+1}} \right)$$

(3.22)

Now we will proceed to express the junction variables in terms of control volume variables.

It is assumed that

$$\bar{w}_i = \frac{1}{2} (w_i + w_{i+1}), \text{ i.e., } w_{i+1} = 2\bar{w}_i - w_i$$

$$\bar{u}_i = \frac{1}{2} (u_i + u_{i+1}), \text{ i.e., } u_{i+1} = 2\bar{u}_i - u_i$$

$$\bar{\rho}_i = \frac{1}{2} (\rho_i + \rho_{i+1}), \text{ i.e., } \rho_{i+1} = 2\bar{\rho}_i - \rho_i$$

Let us define specific internal energy

$$\bar{u}_i = \frac{\int\limits_i^{i+1} A \rho u \, dz}{\int\limits_i^{i+1} A \rho \, dz} = \frac{\bar{U}_i}{A \Delta Z \bar{\rho}_i}.$$

Pressure P_i can be expressed as a function of u_i and ρ_i , i.e.,

$$P_i = P_i(u_i, \rho_i)$$

These variables will take the following form at junction 2:

$$w_2 = 2\bar{w}_1 - w_1$$

$$u_2 = 2\bar{u}_1 - u_1$$

$$\rho_2 = 2\bar{\rho}_1 - \rho_1$$

$$\begin{aligned} P_2 &= P_2(u_2, \rho_2) = P_2(2\bar{u}_1 - u_1, 2\bar{\rho}_1 - \rho_1) \\ &= P_2(\bar{u}_1, \bar{\rho}_2, u_1, \rho_1). \end{aligned}$$

At junction 3:

$$\begin{aligned} w_3 &= 2 \bar{w}_2 - w_2 = 2 \bar{w}_2 - (2 \bar{w}_1 - w_1) \\ &= 2 \bar{w}_2 - 2 \bar{w}_1 + w_1 \end{aligned}$$

Similarly,

$$\begin{aligned} u_3 &= 2 \bar{u}_2 - 2 \bar{u}_1 + u_1 \\ p_3 &= 2 \bar{p}_2 - 2 \bar{p}_1 + p_1 \\ P_3 &= P_3(\bar{u}_2, \bar{u}_1, \bar{p}_2, \bar{p}_1, u_1, p_1) \end{aligned}$$

At junction 4 :

$$\begin{aligned} w_4 &= 2 \bar{w}_3 - 2 \bar{w}_2 + 2 \bar{w}_1 - w_1 \\ u_4 &= 2 \bar{u}_3 - 2 \bar{u}_2 + 2 \bar{u}_1 - u_1 \\ p_4 &= 2 \bar{p}_3 - 2 \bar{p}_2 + 2 \bar{p}_1 - p_1 \\ P_4 &= P_4(\bar{u}_2, \bar{u}_1, u_1, \bar{p}_3, \bar{p}_2, \bar{p}_1, u_1, p_1) \end{aligned}$$

At junction n:

$$\begin{aligned} w_n &= 2 \bar{w}_{n-1} - 2 \bar{w}_{n-2} + 2 \bar{w}_{n-3} - \dots + (-1)^{n-1} w_1 \\ \text{for } n &= 2, 3, 4, \dots, N. \end{aligned}$$

i.e.,

$$w_n = (-1)^{n-1} w_1 + 2 \sum_{K=1}^{n-1} (-1)^{n+K-1} \bar{w}_K$$

for $n = 2, 3, 4, \dots, N$.

Similarly for $n = 2, 3, 4, \dots, N$.

$$u_n = (-1)^{n-1} u_1 + 2 \sum_{K=1}^{n-1} (-1)^{n+K-1} \bar{u}_K$$

$$\rho_n = (-1)^{n-1} \rho_1 + 2 \sum_{K=1}^{n-1} (-1)^{n+K-1} \bar{\rho}_K$$

and $P_n = P_n(\bar{u}_{n-1}, \bar{u}_{n-2}, \dots, \bar{u}_1, \bar{\rho}_{n-1}, \dots, \bar{\rho}_1, u_1, \rho_1)$

Using these expressions the equations 3.20, 3.21 and 3.22 can be written as

$$\dot{\bar{\rho}}_n = \frac{1}{A\Delta Z} [\{ (-1)^{n-1} w_1 + \sum_{K=1}^{n-1} (-1)^{n+K-1} 2 \bar{w}_K \} - \{ (-1)^n w_1 + \sum_{k=1}^n (-1)^{n+k} 2 \bar{w}_K \}] \quad (3.23)$$

$$\dot{\bar{U}}_n = \bar{Q}_n + [(-1)^{n-1} w_1 + \sum_{K=1}^{n-1} (-1)^{n+K} 2 \bar{w}_K] \times [(-1)^{n-1} u_1 + \sum_{K=1}^{n-1} (-1)^{n+K-1} 2 \bar{u}_K] - [(-1)^n w_1 + \sum_{K=1}^n (-1)^{n+k} 2 \bar{w}_K] \times [(-1)^n u_1 + \sum_{K=1}^n (-1)^{n+k} 2 \bar{u}_K]$$

$$\begin{aligned}
 & - \bar{F}_n C_2 \left[\frac{\sum_{K=1}^n (-1)^{n+K} 2 \bar{W}_K}{\sum_{K=1}^n (-1)^n \bar{\rho}_1 + \sum_{K=1}^n (-1)^{n+K} 2 \bar{\rho}_K} - \frac{\sum_{K=1}^n (-1)^{n+K-1} 2 \bar{W}_K}{\sum_{K=1}^{n-1} (-1)^{n+K-1} 2 \bar{\rho}_K} \right] \\
 & + C_3 \cdot \bar{f}_n \frac{\bar{W}_n^3}{2A^2 D_e \bar{\rho}_1^2} \cdot \Delta Z \quad (3.24)
 \end{aligned}$$

$$\begin{aligned}
 \dot{\bar{W}}_n &= \frac{C_1 A}{\Delta Z} P_n(\bar{u}_{n-1}, \bar{u}_{n-2}, \dots, \bar{u}_1, \bar{\rho}_{n-1}, \bar{\rho}_{n-2}, \dots, \bar{\rho}_1, u_1, \rho_1) \\
 & - \frac{C_1 A}{\Delta Z} P_{n+1}(u_n, u_{n-1}, u_{n-2}, \dots, u_1, \bar{\rho}_n, \bar{\rho}_{n-1}, \dots, \bar{\rho}_1, u_1, \rho_1) \\
 & + \frac{r_n}{A \cdot \Delta Z} \times \frac{[(\sum_{K=1}^{n-1} (-1)^{n+K-1} 2 \bar{W}_K)^2]}{[(\sum_{K=1}^{n-1} (-1)^{n+K-1} 2 \bar{\rho}_K)]} \\
 & - \frac{r_n}{A \cdot \Delta Z} \times \frac{[(\sum_{K=1}^n (-1)^{n+K} 2 W_K)^2]}{[(\sum_{K=1}^n (-1)^{n+K} 2 \bar{\rho}_K)]} \\
 & - \bar{f}_n \frac{\bar{W}_n^2}{2A D_e \bar{\rho}_n} \quad (3.25)
 \end{aligned}$$

3.2.4 Solution of the system of equations:

Each control volume is represented by the equations 3.23, 3.24 and 3.25. So for each control volume there will be 3 equations with 3 unknowns. Porsching [10] had pointed out that for any thermal-hydraulic network involving the three basic

conservation equations, an explicit numerical scheme can be formulated which is consistent and stable for some appropriate time-step.

(a) Derivation of the numerical scheme:

Equations 4.13, 4.14 and 4.15 can be written as

$$\dot{\rho}_i = F_j, \quad i = 1, 2, \dots, N \text{ and } j = 1, 2, \dots, N$$

$$\dot{\bar{U}}_i = F_j, \quad i = 1, 2, \dots, N \text{ and } j = N+1, N+2, \dots, 2N$$

$$\dot{\bar{W}}_i = F_j, \quad i = 1, 2, \dots, N \text{ and } j = 2N+1, 2N+2, \dots, 3N$$

Let us define

$$\underline{y} = \text{Vector} [\bar{\rho}_1, \bar{\rho}_2, \dots, \bar{\rho}_N, \bar{U}_1, \bar{U}_2, \dots, \bar{U}_N, \bar{W}_1, \bar{W}_2, \dots, \bar{W}_N]$$

and

$$\underline{F}(t, \underline{y}) = \text{Vector} [F_1, F_2, \dots, F_N, F_{N+1}, F_{N+2}, \dots, F_{2N},$$

$$F_{2N+1}, F_{2N+2}, \dots, F_{3N}]$$

It can be written using these two definitions

$$\dot{\underline{y}} = \underline{F}(t, \underline{y})$$

So the equation to be solved is

$$\dot{\underline{y}} = \underline{F}(t, \underline{y}) \text{ with the initial condition } \underline{y}(0) = \underline{y}_0.$$

The given differential equation can be written as

$$\frac{dy}{dt} = \underline{F}(t, y)$$

$$\begin{aligned} \text{i.e., } \Delta \underline{y}^{n+1} &= \underline{F}^{n+1} \Delta t \\ &= \{\underline{F}^n + \underline{F}^{n+1} - \underline{F}^n\} \Delta t \\ &= \{\underline{F}^n + \Delta \underline{F}^{n+1}\} \Delta t \end{aligned}$$

If we approximate

$$\frac{d\underline{F}}{dt} \Big|_n = \frac{\Delta \underline{F}^{n+1}}{\Delta \underline{y}^{n+1}}$$

$$\text{then } \Delta \underline{F}^{n+1} = \frac{d\underline{F}}{dt} \Big|_n \times \Delta \underline{y}^{n+1}$$

So we now have

$$\Delta \underline{y}^{n+1} = [\underline{F}^n + \frac{d\underline{F}}{dy} \Big|_n \Delta \underline{y}^{n+1}] \Delta t$$

$$\text{i.e., } [I - \frac{d\underline{F}}{dy} \Big|_n \Delta t] \Delta \underline{y}^{n+1} = \underline{F}^n \Delta t$$

The matrix representation of this equation will be

$$\begin{bmatrix} 1 - \Delta t \frac{\partial \dot{\rho}_i}{\partial \bar{\rho}_i} & -\Delta t \frac{\partial \dot{\rho}_i}{\partial \bar{U}_i} & -\Delta t \frac{\partial \dot{\rho}_i}{\partial \bar{W}_i} \\ -\Delta t \frac{\partial \dot{U}_i}{\partial \bar{\rho}_i} & 1 - \Delta t \frac{\partial \dot{U}_i}{\partial \bar{U}_i} & -\Delta t \frac{\partial \dot{U}_i}{\partial \bar{W}_i} \\ -\Delta t \frac{\partial \dot{W}_i}{\partial \bar{\rho}_i} & -\Delta t \frac{\partial \dot{W}_i}{\partial \bar{U}_i} & 1 - \Delta t \frac{\partial \dot{W}_i}{\partial \bar{W}_i} \end{bmatrix} \begin{bmatrix} \dot{\rho}_i \\ \dot{U}_i \\ \dot{W}_i \end{bmatrix} = \begin{bmatrix} \dot{\rho}_i \\ \dot{U}_i \\ \dot{W}_i \end{bmatrix} \Delta t$$

Before evaluating these derivatives let us first establish a few identities which will be used for the evaluation of the derivatives. It has been shown that

$$\rho_n = (-1)^{n-1} \rho_1 + 2 \sum_{K=1}^{n-1} (-1)^{n+K-1} \rho_K$$

So $\frac{\partial \rho_n}{\partial \bar{\rho}_j} = (-1)^{n+j-1} \cdot 2$

and $\frac{\partial \rho_{n+1}}{\partial \bar{\rho}_j} = (-1)^{n+j} \cdot 2$

Similarly,

$$\frac{\partial \bar{u}_n}{\partial \bar{u}_j} = (-1)^{n+j-1} \cdot 2$$

and

$$\frac{\partial \bar{u}_{n+1}}{\partial \bar{u}_j} = (-1)^{n+j} \cdot 2$$

Also

$$\bar{u}_j = \frac{\bar{U}_j}{A \bar{\rho}_j \Delta Z}$$

i.e., $\frac{\partial \bar{u}_j}{\partial \bar{U}_j} = \frac{1}{A \bar{\rho}_j \Delta Z}$

Using these identities and taking the derivatives of equations 3.23, 3.24 and 3.25 with respect to $\bar{\rho}_i$, \bar{U}_i and \bar{W}_i for $n = i$ and utilizing the following three notations.

$$w_m = (-1)^{m-1} w_1 + 2 \sum_{K=1}^{m-1} (-1)^{m+K-1} \bar{w}_K$$

$$u_m = (-1)^{m-1} u_1 + 2 \sum_{K=1}^{m-1} (-1)^{m+K-1} \bar{u}_K$$

$$\rho_m = (-1)^{m-1} \rho_1 + 2 \sum_{K=1}^{m-1} (-1)^{m+K-1} \bar{\rho}_K$$

We get

$$\frac{\partial \dot{\bar{\rho}}_i}{\partial \bar{\rho}_i} = 0$$

$$\frac{\partial \dot{\bar{\rho}}_i}{\partial \bar{U}_i} = 0$$

$$\frac{\partial \dot{\bar{\rho}}_i}{\partial \bar{W}_i} = - \frac{2}{A \cdot \Delta Z}$$

$$\begin{aligned}\frac{\partial \dot{\bar{U}}_i}{\partial \bar{\rho}_i} &= -C_2 \left(\frac{\partial \bar{P}_i}{\partial \bar{\rho}_i} \right) \left(\frac{W_{i+1}}{\rho_{i+1}} - \frac{W_i}{\rho_i} \right) \\ &\quad + C_2 \cdot \bar{P}_i \cdot 2 \cdot \frac{W_{i+1}}{\rho_{i+1}} - \bar{f}_i \cdot C_3 \frac{\bar{W}_i^3 \cdot \Delta Z}{A^2 \cdot D_e \cdot \bar{\rho}_i}\end{aligned}$$

$$\frac{\partial \dot{\bar{U}}_i}{\partial \dot{\bar{U}}_i} = -\frac{2W_{i+1}}{A \cdot \Delta Z \cdot \bar{\rho}_i} - C_2 \left(\frac{\partial \bar{P}_i}{\partial \bar{U}} \right)_i \left(\frac{W_{i+1}}{\rho_{i+1}} - \frac{W_i}{\rho_i} \right)$$

$$\frac{\partial \dot{\bar{U}}_i}{\partial \bar{W}_i} = -2u_{i+1} - C_2 \frac{2 \bar{P}_i}{\rho_{i+1}} + \frac{3}{2} \cdot C_3 \frac{\bar{f}_i \bar{W}_i^2 \Delta Z}{A^2 \cdot D_e \cdot \bar{\rho}_i^2}$$

$$\frac{\partial \dot{\bar{W}}_i}{\partial \bar{\rho}_i} = -C_1 \frac{A}{\Delta Z} 2 \left(\frac{\partial P}{\partial \rho} \right)_{i+1} + \frac{r_{i+1}}{A \cdot \Delta Z} \cdot \frac{W_{i+1}^2}{\rho_{i+1}} + \bar{f}_i \frac{W_i^2}{2 A D_e \bar{\rho}_i^2}$$

$$\frac{\partial \dot{\bar{W}}_i}{\partial \bar{U}_i} = -C_1 \frac{2}{\Delta Z^2 \bar{\rho}_i} \left(\frac{\partial P}{\partial U} \right)_{i+1}$$

$$\frac{\partial \dot{\bar{W}}_i}{\partial \bar{W}_i} = -\frac{\bar{f}_i \bar{W}_i}{A \cdot D_e \cdot \bar{\rho}_i} - \frac{4 \cdot 4_{i+1} W_{i+1}}{A \cdot \Delta Z \cdot \rho_{i+1}}$$

Using these values in the above 3×3 matrix the values of $\Delta \bar{\rho}_i$, $\Delta \bar{U}_i$ and $\Delta \bar{W}_i$ can be calculated for each control volume and knowing these values ρ_i^{n+1} , \bar{U}_i^{n+1} and \bar{W}_i^{n+1} can be determined by using

$$\bar{\rho}_i^{n+1} = \bar{\rho}_i^n + \Delta \bar{\rho}_i$$

$$\bar{U}_i^{n+1} = \bar{U}_i^n + \Delta \bar{U}_i$$

$$\bar{W}_i^{n+1} = \bar{W}_i^n + \Delta \bar{W}_i$$

Once $\bar{\rho}_i^{n+1}$, \bar{U}_i^{n+1} and \bar{W}_i^{n+1} are known, other parameters

can be easily determined.

CHAPTER 4

DESCRIPTION OF THE COMPUTER CODE

4.1 Input Variables:

The input to the computer code is fairly simple. Some of the data can be directly taken from the steam table. But other data have to be generated by polynomial regression using the data of compressed liquid (water).

The required input data cards are listed below. The units of each parameter and their input format are also included.

Card No.	Variable	Value	Format
1-118	AGUAS (I,1)	Saturation pressure in psi	F 10.4
	AGUAS (I,2)	Saturation temperature in °F	F 10.4
	AGUAS (I,3)	Sp. Vol. of liquid in ft ³ /lbm.	F 10.4
	AGUAS (I,4)	Sp. Vol. of vapour in ft ³ /lbm.	F 10.4
	AGUAS (I,5)	Sp. enthalpy of liquid in Btu/lbm	F 10.4
	AGUAS (I,6)	Sp. enthalpy of vapour in Btu/lbm	F 10.4

The cards are in decreasing order of saturation pressure.

119-126 ((AGUAC (I,J), J = 1, 12), I = 1, 4)

Format is 6E12.6 for each card and there will be 6 values on each card.

J = 12 different values of temperature

I = 1 Temperature

I = 2 Constant part

I = 3 Coefficient of P

I = 4 Coefficient of P^2

127 FREGB Limits of quality regions 6F 10.4
6 values

128-166 COEFB(I,J) Interpolated values 5E 15.6
((COEFB(I,J), J = 1, 15), I = 1, 13)
5 values on each card.

I=13 Quality for the curve

J=1,15 Indicates the pressure set to be used.

I=1-6 A for each set

I=7-12 B for each set

(COEFB(13,K), K=1,15) Quality of each of the 15 curves of Baroczy plot.

167-168 GAMAT Gamma factor 7F 10.4
((GAMAT(I,J), J=1,7), I=1,2)
J=1 Indicates pressure
J=2 Indicates gama factor

Card No.	Variable	Value	Format
169	GNOME	Name of the programme	20A
170	NVC	No. of control volume	I3
	NMCL	Maximum No. of iterations	I3
	IESCR	Output option = 0, Print final value = 1, Print all iterations = 2, Print all details	I1
	PRECQ	Precision required	F10.3
	GRAV	Acceleration due to gravity	F10.3
171	NTP	No.of U-tubes in primary	I7
	MALHA	Type of pitch = 1, Square pitch = 2, Triangular pitch	I1
	ATTC	Total heat transfer area (ft ²)	F10.2
	DEX	External diameter (inches)	F10.2
	DIN	Internal diameter(inches)	F10.2
	PASSO	Spacing between tubes (inches)	F10.2
	COEFF	Form factor	F10.2
172	PPJ(1)	Inlet steam pressure (Psi)	F10.2
	TPJ(1)	Inlet steam temperature (°F)	F10.2

Card No.	Variable	Value	Format
	HPJ (l)	Inlet steam enthalpy (Btu/lbm)	F10.2
	PSP	Estimated primary pressure (Psi)	F10.2
	WP	Inlet flow rate in primary (lbm/hr)	E12.6
173	PEAA	Pressure of feed water (Psi)	F10.2
	TEAA	Temperature of feed water ($^{\circ}$ F)	F10.2
	HEAA	Enthalpy of feed water (Btu/lbm)	F10.2
	PSS	Exit pressure (Psi)	F10.2
	XExit	Quality at exit	F10.2
	WS	Flow rate of feed water (lbm/hr)	E12.6
174	QTOT	Total heat transfer rate (Btu/hr)	E12.6
175	OP	Calculation option	I1
		= 1, calculate only the steady state values	
		# 1, calculate both steady state values and transients.	
176-183	UFVAC(I,J)	Polynomials expressing internal energy (u) as a function of sp.vol.(v)	5X, F7.1, 5X, 3E16.5
		((UFVAC(I,J), J=1,4), I=1,8)	
		4 values on each card.	

Card No.	Variable	Value	Format
	I = 8	different values at pressure	
	J = 1	Pressure	
	J = 2	Constant part	
	J = 3	Coefficient of v	
	J = 4	Coefficient of v ²	
	The cards are in increasing order of the pressure. These are for compressed water.		
184-191	VFUAC(I,J)	Polynomials expressing sp.vol.(v) as a function of internal energy (u)	5X, F7.1, 5X, 3E16.5
	((VFUAC(I,J), J=1,4), I=1,8)		
	4 values on each card.		
	I = 8	different pressure values	
	J = 1	Pressure	
	J = 2	Constant part	
	J = 3	Coefficient of u	
	J = 4	Coefficient of u ²	
	The cards are in increasing order of the pressure. These are for compressed water.		
192	Time (Sec)	Duration over which the transient has to be calculated.	No format is needed
	NIT	No. of intervals	No format is needed

Card No.	Variable	Value	Format
193-207	VFPH (I,J)	Polynomials expressing sp.vol. (v) as a function of pressure (P) at constant enthalpy(h)	3X, F6.1, 3E19.7
		((VFPH (I,J), J=1,4), I=1,15)	
		4 values on each card.	
	I = 15	different enthalpy values.	
	J = 1	Enthalpy	
	J = 2	Constant part	
	J = 3	Coefficient of P	
	J = 4	Coefficient of P ²	
	The cards are in increasing order of the enthalpy. These are for compressed water.		
208	VEPPJ (2)	Sp.Vol. of compressed water at the inlet condition of the pre- heater of primary circuit.	No format is needed
209	VESPJ (1)	Sp. volume of water at the inlet condition of the preheater of second- ary circuit.	No format is needed

4.2 Steady state calculation:

For calculating the steady state values, i.e., the starting values for transient calculation the computer code and the model developed by A.C. Pinto [7] are used.

4.2.1 Flow-chart :

The procedure involved in the above computer code is given in the form of a flow-chart in figure 4.1. The function of various subroutines will be discussed in the next section.

4.2.2 Subroutines [7]:

(a) CPAGC - It calculates specific heat C_p of compressed water at constant pressure as a function of temperature ($^{\circ}\text{F}$) at various pressure range. The unit of specific heat is $\text{Btu/lb-}^{\circ}\text{F}$.

(i) $C_p = 0.14931 \cdot 10^{-5} T^2 - 0.45187 \cdot 10^{-3} T + 1.0241$ for
 $P \leq 1500 \text{ Psi.}$

(ii) 1500 Psi : $P \leq 2500 \text{ Psi}$

$$C_p = 0.90724 \cdot 10^{-6} T^2 - 0.23174 \cdot 10^{-3} T + 1.0049, \quad T \leq 300^{\circ}\text{F}$$

$$C_p = 0.38132 \cdot 10^{-7} T^3 - 0.453 \cdot 10^{-4} T^2 - 0.18281 \cdot 10^{-1} T - 1.4375 \quad \text{for } T > 300^{\circ}\text{F.}$$

(iii) $2500 \text{ Psi} < P \leq 3500 \text{ Psi}$

$$C_p = 0.90941 \cdot 10^{-6} T^2 - 0.24668 \times 10^{-3} T + 1.0028 \quad \text{for } T \leq 300^{\circ}\text{F}$$

$$C_p = 0.47072 \cdot 10^{-6} T^2 - 0.31944 \cdot 10^{-2} T + 1.5651 \quad \text{for } 300^{\circ}\text{F} < T \leq 620^{\circ}\text{F}$$

$$C_p = 0.22404 \cdot 10^{-6} T^3 - 0.10377 \cdot 10^{-3} T^2 - 0.13194 T + 69.772 \quad \text{for } T > 620^{\circ}\text{F.}$$

- (b) CPAGS - It calculates specific heat C_p of saturated water as a function of temperature T .

$$C_p = 0.10313 \cdot 10^{-5} T^2 - 0.25129 \cdot 10^{-3} T + 1.0125 \text{ for } T \leq 410^{\circ}\text{F}$$

$$C_p = 0.13446 \cdot 10^{-4} T^2 - 0.11339 \cdot 10^{-1} T + 3.4878$$

for $410 < T \leq 630^{\circ}\text{F}$

$$C_p = 0.21005 T - 11.543, \quad 630 < T \leq 660^{\circ}\text{F}$$

$$C_p = 0.58005 T - 35.97, \quad 660 < T \leq 680^{\circ}\text{F}$$

$$C_p = 0.20068 T - 132.97, \quad T > 680^{\circ}\text{F}$$

- (c) CTAGC - It calculates the conductivity (k) of compressed water in Btu/hr-ft- $^{\circ}\text{F}$ as a function of pressure (psi) and temperature ($^{\circ}\text{F}$).

- (i) $P \leq 1500$ Psi

$$k = 0.1131 \cdot 10^{-5} T^2 + 0.64326 \cdot 10^{-3} T + 0.30963$$

- (ii) $1500 < P \leq 2500$ Psi

$$k = -0.11059 \cdot 10^{-5} T^2 + 0.63854 \cdot 10^{-3} T + 0.31182$$

- (iii) $2500 < P \leq 3500$ Psi

$$k = -0.11495 \cdot 10^{-5} T^2 + 0.67117 \cdot 10^{-3} T + 0.3105.$$

- (d) CTAGC - It calculates the conductivity (k) of saturated water as a function of temperature (T).

$$k = -0.24173 \cdot 10^{-5} T^2 + 0.99835 \cdot 10^{-3} T + 0.28862$$

for $T \leq 100 {}^{\circ}\text{F}$.

$$k = -0.10408 \cdot 10^{-5} T^2 + 0.5628 \cdot 10^{-3} + 0.32132$$

for $100 < T \leq 400 {}^{\circ}\text{F}$.

$$k = -0.20081 \cdot 10^{-5} T^2 + 0.15749 \cdot 10^{-2} T + 0.06624$$

for $T > 400 {}^{\circ}\text{F}$

- (e) CTMTP - It calculates the conductivity (k) of the material of the tube. The material chosen in this problem is Inconel-718.

$$k = 57.78 (-1.98 \times 10^{-6} T^2 + 8.91 \times 10^{-4} T + 0.151)$$

where k is in $\text{Btu}/\text{hr} \cdot \text{ft} \cdot {}^{\circ}\text{F}$ and T in ${}^{\circ}\text{C}$.

- (f) FTMDP - It calculates the multiplication factor needed to evaluate two-phase frictional pressure drop. For this Baroczy's plot [9] is used. The X-axis of this log-log plot is divided into 6 regions and the segments in each region is assumed to be linear such that

$$\frac{\phi^2}{L_o} = \text{Exp} (A + B \ln I).$$

A and B are determined using the plot. The six regions are:

Region I : $0.00001 \leq I \leq 0.001$

Region II : $0.001 < I \leq 0.003$

Region III : $0.003 < I \leq 0.007$

Region IV : $0.007 < I \leq 0.03$

Region V : $0.03 < I \leq 0.1$

Region VI : $0.1 < I \leq 1.0$

$$\text{where } I = (\mu_L/\mu_V)^{0.2} (\epsilon_L/\epsilon_V)$$

(g) QFOCV - It calculates F, S and σ to be used in Chen's correlation.

$$F = \text{Exp} [0.60358 + 0.21681 \ln(x_{tt}^{-1})], \quad 0.1 \quad x_{tt}^{-1} \quad 0.2$$

$$F = \text{Exp} [0.94034 + 0.42604 \ln(x_{tt}^{-1})], \quad 0.2 \quad x_{tt}^{-1} \quad 0.6$$

$$F = \text{Exp} [1.0359 + 0.61316 \ln(x_{tt}^{-1})], \quad 0.6 \quad x_{tt}^{-1} \quad 2.0$$

$$F = \text{Exp} [0.96332 + 0.71791 \ln(x_{tt}^{-1})], \quad 2.0 \quad x_{tt}^{-1} \quad 100.0$$

$$S = 0.43321 \cdot 10^{-10} B^2 - 0.10254 \cdot 10^{-4} B + 0.97877$$

$$\text{For } 14990 \leq B \leq 1.75$$

$$S = 0.54595 \cdot 10^{-11} B^2 - 0.33653 \cdot 10^{-5} B + 0.65916$$

$$\text{For } 10^5 < B \leq 3.0 \times 10^5$$

$$S = 0.10265 \cdot 10^{-11} B^2 - 0.99733 \cdot 10^{-6} B + 0.34334$$

$$\text{For } 3 \times 10^5 < B \leq 5 \times 10^5$$

$$S = 0.11075 \cdot 10^{-12} B^2 - 0.18338 \cdot 10^{-6} B + 0.16406$$

For $5 \times 10^5 < B \leq 7 \times 10^5$

$$S = 0.9, \quad \text{For } B > 7 \times 10^5$$

$$\text{where } B = Re_1 \cdot F^{1.25}$$

$$\sigma = 0.157 \cdot 10^{-8} P^2 - 0.36872 \cdot 10^{-5} P + 0.0033934$$

For $P \leq 1000 \text{ Psi}$

$$\sigma = 0.2023 \cdot 10^{-9} P^2 - 0.1402 \cdot 10^{-5} P + 0.0024308$$

For $1000 < P \leq 3000 \text{ Psi}$

where σ is in lbf/ft .

- (h) TLSUB - It determines the temperature of compressed water for a given pressure (P , psi) and specific enthalpy (H , Btu/lbm).

$$H = 0.26127 \cdot 10^{-2} P + 68.0349, \quad T = 100 \text{ } ^\circ\text{F}$$

$$H = 0.22714 \cdot 10^{-2} P + 167.946, \quad T = 200 \text{ } ^\circ\text{F}$$

$$H = 0.18834 \cdot 10^{-2} P + 269.445, \quad T = 300 \text{ } ^\circ\text{F}$$

$$H = 0.49075 \cdot 10^{-7} P^2 + 0.10506 \cdot 10^{-2} P + 374.7088, \quad T = 400 \text{ } ^\circ\text{F}$$

$$H = 0.10528 \cdot 10^{-6} P^2 - 0.56072 \cdot 10^{-3} P + 488.1221, \quad T = 500 \text{ } ^\circ\text{F}$$

$$H = 0.81068 \cdot 10^{-6} P^2 - 0.84505 \cdot 10^{-2} P + 628.158, \quad T = 600 \text{ } ^\circ\text{F}$$

$$H = 0.13553 \cdot 10^{-5} P^2 - 0.13685 \cdot 10^{-1} P + 666.845, \quad T = 620 \text{ } ^\circ\text{F}$$

$$H = 0.18628 \cdot 10^{-5} P^2 - 0.20086 \cdot 10^{-1} P + 711.776, \quad T = 640 \text{ } ^\circ\text{F}$$

$$H = 0.53821 \cdot 10^{-5} P^2 - 0.46992 \cdot 10^{-1} P + 794.942, \quad T = 660 \text{ } ^\circ\text{F}$$

$$H = 0.75397 \cdot 10^{-5} P^2 - 0.7298 \cdot 10^{-1} P + 896.170, \quad T = 680 \text{ } ^\circ\text{F}$$

$$H = 0.19416 \cdot 10^{-4} P^2 - 0.16793 \cdot P + 1104.3, \quad T = 690 \text{ } ^\circ\text{F}$$

$$H = 0.24845 \cdot 10^{-4} P^2 - 0.22748 \cdot P + 1274.58, \quad T = 700 \text{ } ^\circ\text{F}.$$

(ii) VIAGC - It determines the viscosity (μ) of compressed water in lbm/Hr-ft as a function of pressure (p, psi) and temperature (T, $^\circ\text{F}$).

(i) $P \leq 1500 \text{ Psi}$

$$\mu = 0.3705 \cdot 10^{-3} T^2 - 0.87236 \cdot 10^{-1} T + 6.6531$$

for $T \leq 110 \text{ } ^\circ\text{F}$

$$\mu = -0.66532 \cdot 10^{-7} T^3 + 0.66982 \cdot 10^{-4} T^2 - 0.23742 \cdot 10^{-1} T$$

$+ 3.3519$ for $110 \text{ } ^\circ\text{F} < T \leq 400 \text{ } ^\circ\text{F}$

$$\mu = 0.14575 \cdot 10^{-5} T^2 - 0.20341 \cdot 10^{-2} T + 0.90965$$

for $T > 400 \text{ } ^\circ\text{F}$

(ii) $1500 < P \leq 2500$ Psi

$$\mu = 0.36496 \cdot 10^{-3} T^2 - 0.86013 \cdot 10^{-1} T + 6.5907, \quad T \leq 110 {}^\circ F$$

$$\begin{aligned} \mu = & -0.65878 \cdot 10^{-7} T^3 + 0.66302 \cdot 10^{-4} T^2 - 0.23542 \cdot 10^{-1} T \\ & + 3.3435, \quad 110 {}^\circ F < T \leq 400 {}^\circ F \end{aligned}$$

$$\mu = 0.11304 \cdot 10^{-5} T^2 - 0.17363 \cdot 10^{-2} T + 0.84679, \quad T > 400 {}^\circ F$$

(iii) 2500 Psi $< P \leq 3500$ Psi

$$\mu = 0.35894 \cdot 10^{-3} T^2 - 0.84719 \cdot 10^{-1} T + 6.5258, \quad T \leq 110 {}^\circ F$$

$$\begin{aligned} \mu = & -0.65076 \cdot 10^{-7} T^3 - 0.65502 \cdot 10^{-4} T^2 - 0.23311 \cdot 10^{-1} T \\ & + 3.3325, \quad 110 < T \leq 400 {}^\circ F \end{aligned}$$

$$\mu = 0.52496 \cdot 10^{-6} T^2 - 0.11349 \cdot 10^{-2} T + 0.70403, \quad T > 400 {}^\circ F$$

(j) VIAGS - It determines the viscosity of saturated water

(μ) in lb/Hr-ft as a function of temperature (T).

$$\mu = 0.37664 \cdot 10^{-3} T^2 - 0.88541 \cdot 10^{-1} T + 6.7181, \quad T \leq 110 {}^\circ F$$

$$\begin{aligned} \mu = & -0.67639 \cdot 10^{-7} T^3 + 0.68025 \cdot 10^{-4} T^2 - 0.24029 \cdot 10^{-1} T \\ & + 3.3665, \quad 110 {}^\circ F < T \leq 400 {}^\circ F \end{aligned}$$

$$\mu = 0.29905 \cdot 10^{-6} T^2 - 0.87608 \cdot 10^{-3} T + 0.62286, \quad T > 400 {}^\circ F$$

(k) VIVAS - It calculates the viscosity of saturated vapour
in lbm/Hr-ft as a function of pressure (psi).

$$\mu = 1.15826 (-0.24353 \cdot 10^{-8} P^2 + 0.13778 \cdot 10^{-4} P + 0.029109)$$

4.3 Transient calculation:

The details of the computer programme developed for simulating the transients of the steam generator has been discussed in the next section.

4.3.1 Flow chart:

The logic of the program is presented in the form of a flow diagram in figure 4.2.

4.3.2 Subroutines:

- (a) SOLUC - This subroutine calls a few other subroutines and simulates the transients. The function of this subroutine is given in the form of a flow diagram in figure 4.3.
- (b) DPRER - It determines $(\frac{\partial P}{\partial \mu})_u$ for both compressed and saturated water. To evaluate this the following relationship is made use of.

$$(\frac{\partial P}{\partial \mu})_u = -\frac{1}{\mu^2} (\frac{\partial P}{\partial v})_u$$

(i) Compressed water:

For compressed water the specific volume (v) was expressed as a function of internal energy (u) at different pressures using the data from the compressed water table of Ref. 11. The polynomials are of the form

$$v = a + bu + cu^2$$

where a , b and c are:

Pressure (Psi)	a	b	c
400.0	0.15991E-01	0.90211E-06	0.16408E-07
600.0	0.15979E-01	0.92847E-06	0.16303E-07
800.0	0.15987E-01	0.40455E-06	0.17907E-07
1000.0	0.15974E-01	0.46761E-06	0.17698E-07
1500.0	0.15945E-01	0.58317E-06	0.17275E-07
2000.0	0.16044E-01	-0.20277E-05	0.23350E-07
2500.0	0.16176E-01	-0.44908E-05	0.27727E-07
3000.0	0.16503E-01	-0.93308E-05	0.35265E-07

To evaluate the required derivative the range of pressure between which the known pressure exists is first determined. Let us assume that the lower limits is P_{l_0} and upper limit is P_u . Corresponding to these two pressures the specific volumes v_{l_0} and v_u are determined using the appropriate polynomial. The required derivative will be

$$\left(\frac{\partial P}{\partial \rho} \right)_u = \frac{P_{l_0} - P_u}{-2(v_{l_0} - v_u)}$$

(ii) Saturated water:

For saturated water two other pressures are selected such that they are on either side of the known pressure, equidistant from the known pressure and do not differ very much from the known pressure. At these two pressures the

specific volumes and hence the densities are determined and then the required derivative is calculated by expressing it in finite difference form.

The error introduced by this technique is partly due to the fact that the slope of the chord differs slightly from the slope of the tangent at the mid-point of the arc, and partly due to the small difference between adjacent variables.

(c) DPRU - This subroutine determines $(\frac{\partial P}{\partial u})_P$. The technique followed in this subroutine is same as that described for the subroutine DPRER. But in this case the internal energy (u) is expressed as a function of specific volume (v) for the compressed water. The polynomials are of the form

$$u = a + bv + c v^2$$

where a, b and c are:

Pressure (Psi)	a	b	c
400.0	- 0.14297E+05	0.15499E+07	- 0.40931E+08
600.0	- 0.14353E+05	0.15575E+07	- 0.41179E+08
800.0	- 0.82765E+04	0.84810E+06	- 0.20534E+08
1000.0	- 0.83259E+04	0.85421E+06	- 0.20716E+08
1500.0	- 0.84463E+04	0.86913E+06	- 0.21161E+08
2000.0	- 0.47179E+04	0.45091E+06	- 0.95155E+07

2500.0	- 0.34271E+04	0.31700E+06	- 0.61180E+07
3000.0	- 0.25483E+04	0.22901E+06	- 0.39811E+07

(d) NEWTON - This subroutine determines the quality of steam using Newton-Rapshon's method. It utilizes the following four polynomials which are obtained by fitting curves for the saturation pressure of water. The following polynomials are valid in the range $401.7 \leq P \leq 2532.4$ psi.

$$v_f = 0.1745921 \times 10^{-1} + 0.5229798 \times 10^{-5} P - 0.1625896 \times 10^{-8} P^2 \\ + 0.5551606 \times 10^{-12} P^3.$$

$$v_g = 0.1967797 \times 10^{+1} - 0.2710660 \times 10^{-2} P + 0.1436388 \times 10^{-5} P^2 \\ - 0.2599688 \times 10^{-9} P^3.$$

$$u_f = 0.3178337 \times 10^3 + 0.3054259 P - 0.1020149 \times 10^{-3} P^2 \\ + 0.17564660 \times 10^{-7} P^3.$$

$$u_g = 0.1120552 \times 10^4 + 0.4207413 \times 10^{-2} P - 0.1494585 \times 10^{-4} P^2 \\ - 0.4154948 \times 10^{-9} P^3$$

$$\text{The quality } X = \frac{u - u_f}{u_g - u_f} = \frac{v - v_f}{v_g - v_f}$$

$$\text{i.e., } u(v_g - v_f) - v(u_g - u_f) + u_g v_f - u_f v_g = 0$$

In the L.H.S. of this expression u and v are known and hence constant. All variables other than these two are function of pressure. So pressure can be calculated from this equation. For this purpose Newton-Rapshon's method is used. Once pressure is known u_f and u_g can be calculated from the above polynomials and hence the quality X can be determined.

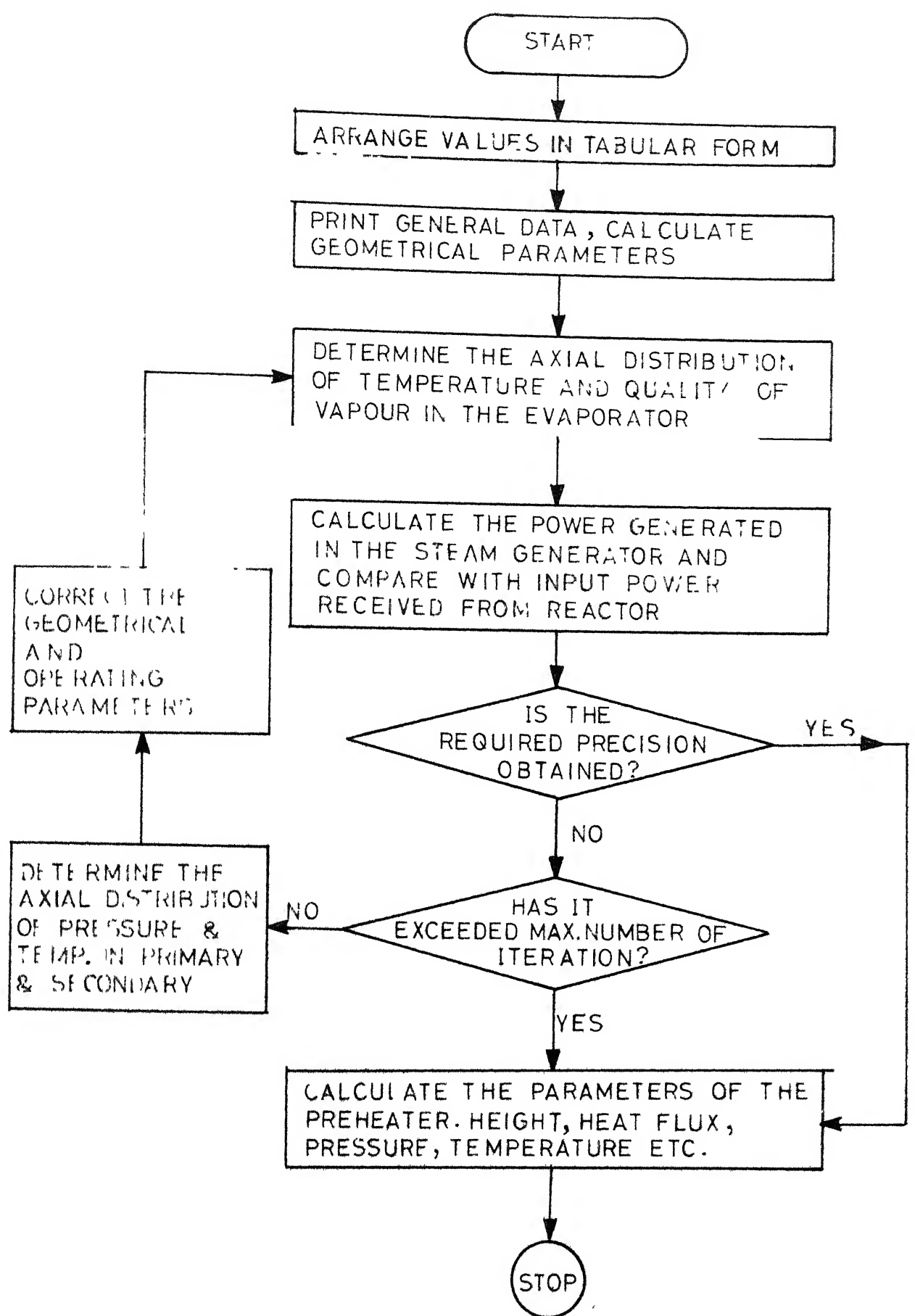
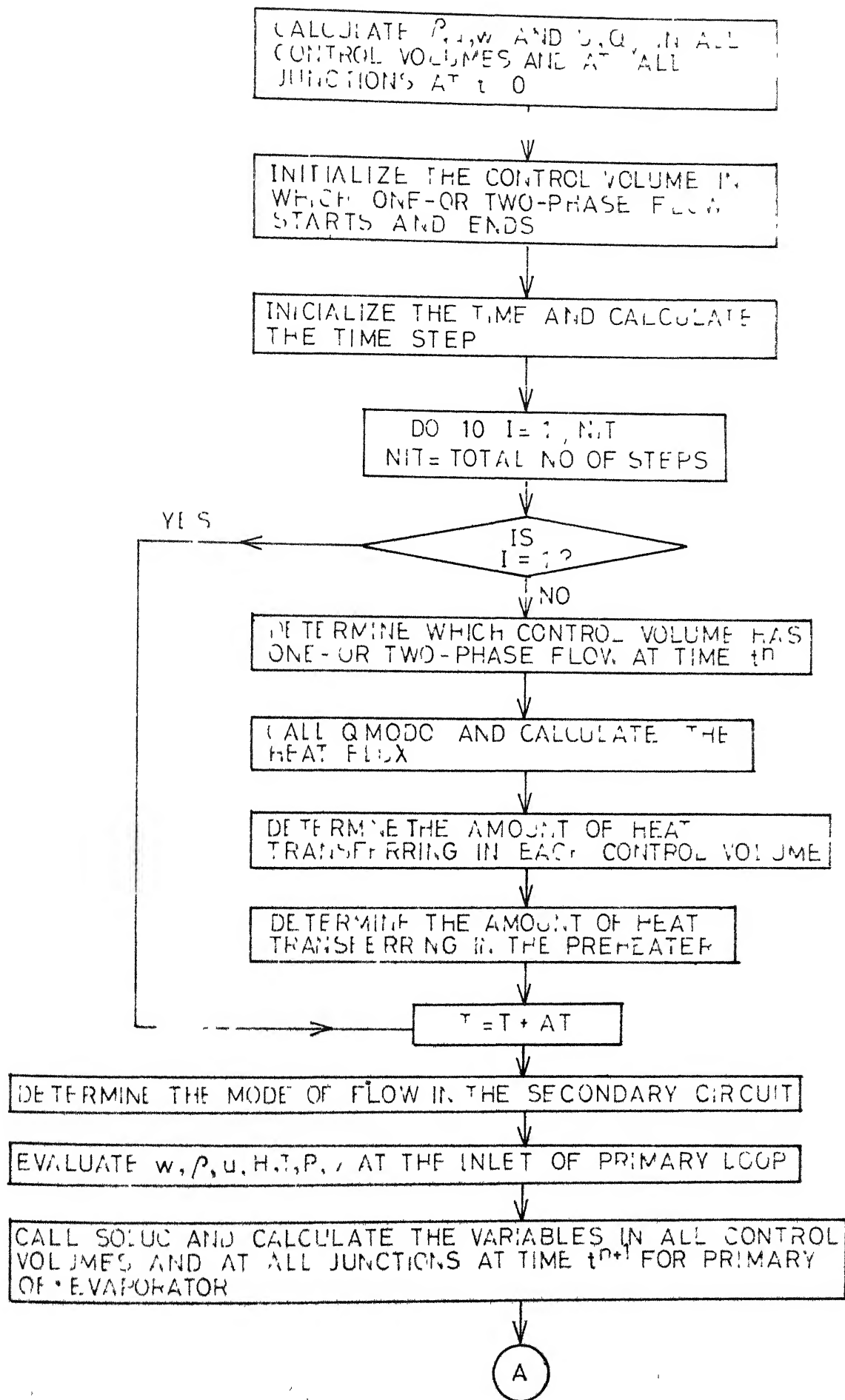
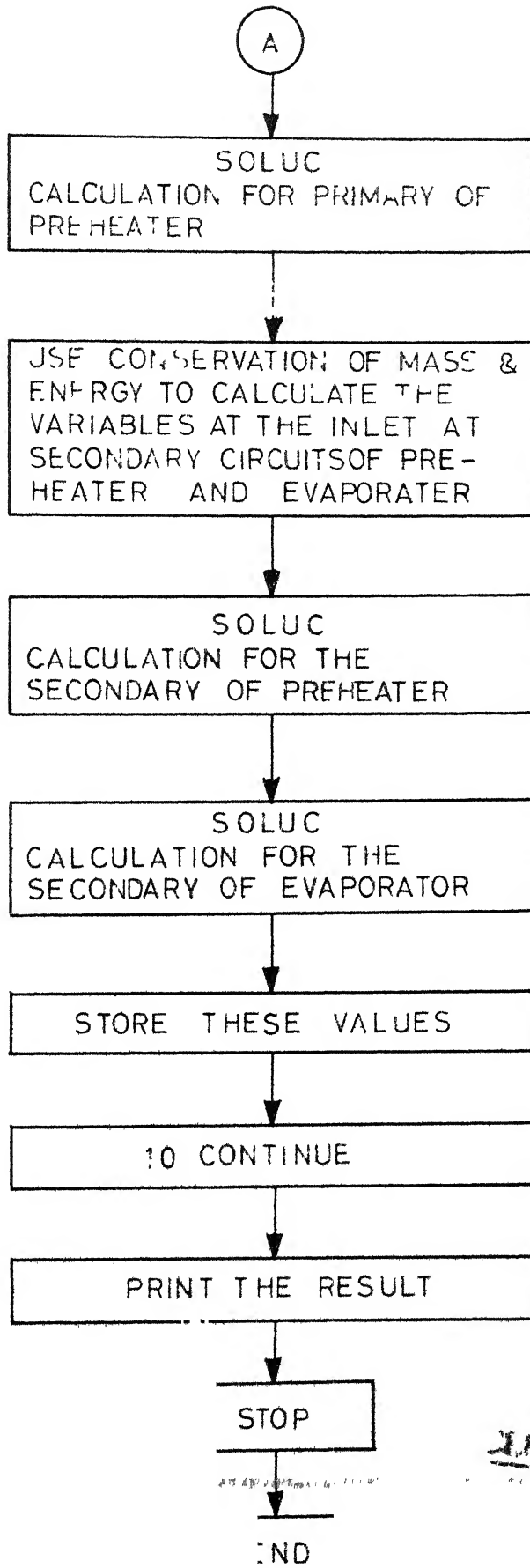
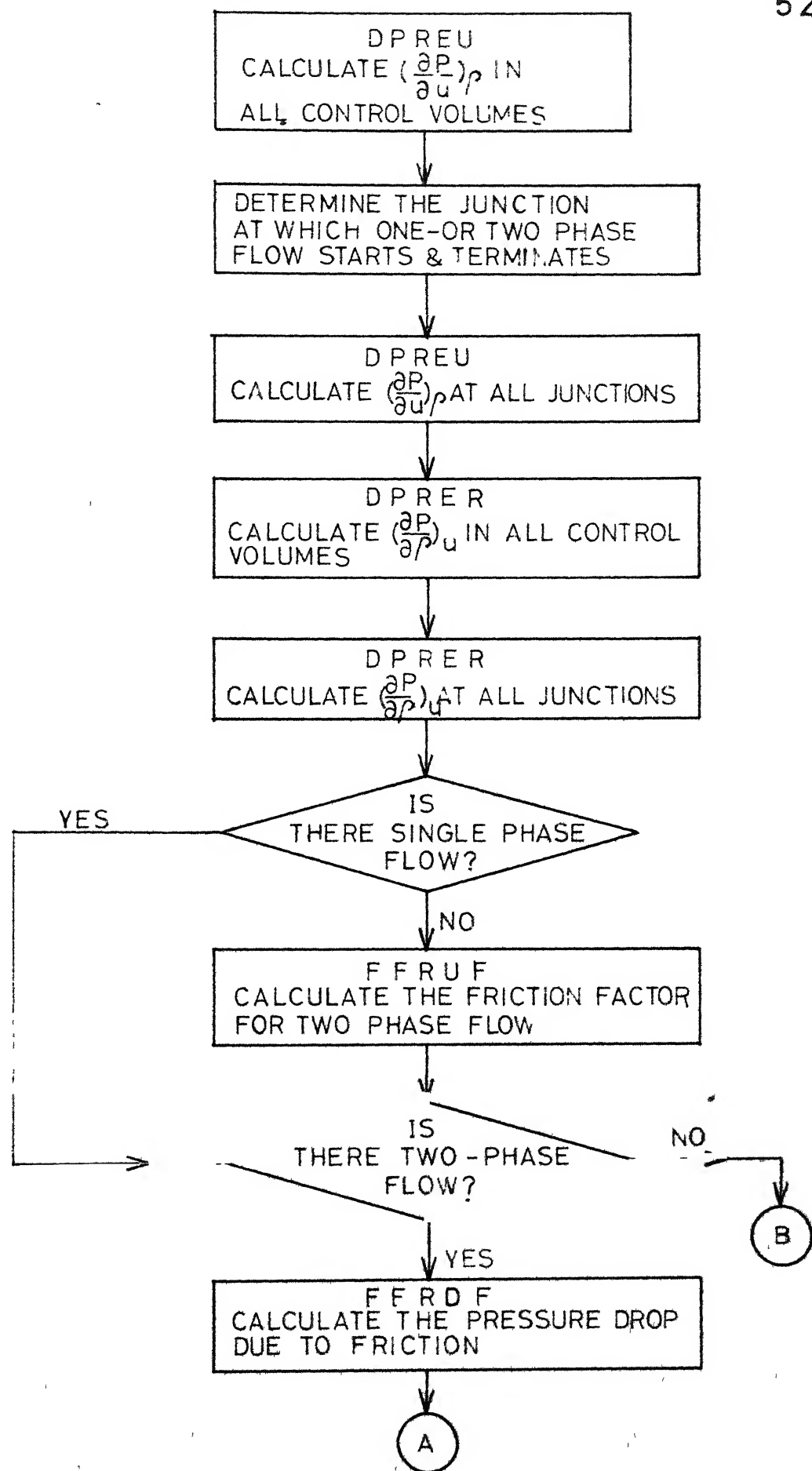


Fig. 4.1 Flow chart of the computer programme calculating the steady state values.





APLII
FINAL LIBRARY
621 23



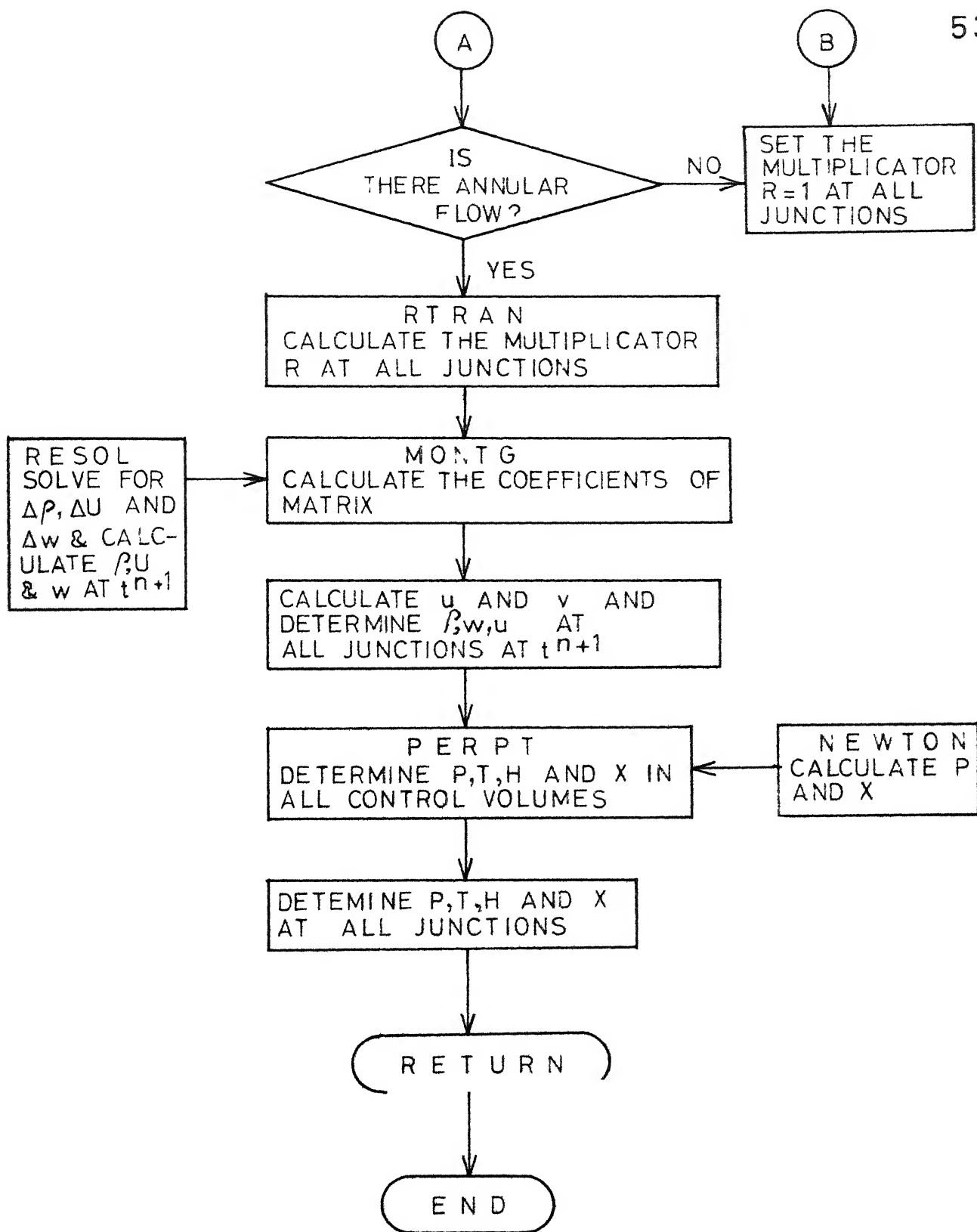


Fig. 4-3 Flow chart of the subroutine SOLUC

CHAPTER 5

RESULTS

5.1 Results and Discussions:

This chapter deals with the results obtained using the computer code developed in this present work. The results will be discussed in details in the following two sections.

5.1.1 Steady state values:

The steady state values which are required for transient analysis were obtained using the computer code developed by A.C. Pinto [7]. These steady state operating values which symbolize the steam generator chosen for transient analysis in the present work are given in appendix C.

5.1.2 Transient values:

The results of the transient analysis are represented in graphical forms. Figures 5.1a through 5.6d indicate the transient behaviour of the steam generator under perturbed conditions.

Figures 5.1a through 5.1d represent the change of variables at the exist of the evaporator of the secondary circuit due to a 5.0 % increment in the mass flow rate at the inlet of the primary circuit. This increase in mass flow rate in the primary circuit will enhance the heat transfer from the primary to the secondary circuit. So the temperature in the secondary circuit

will increase and this will raise the quality. Increase in quality means that there is more vapour and the mass flow rate of vapour is higher. Thus the pressure will rise because there is more vapor and the total mass (liquid and vapor) flow rate will increase.

Figures 5.2a through 5.2d indicate the effect of reducing pressure by 30.0 % at the inlet of the primary circuit. When pressure is reduced by such a large value there will be two-phase flow in the primary circuit and this will increase the heat transfer coefficient from the bulk of the fluid to the tube wall. This essentially will lead to an increase in heat transfer to the secondary circuit and thus the same phenomena as in figures 5.1a through 5.1d will occur.

In figures 5.3a through 5.3d the effect of increasing the internal energy of the primary liquid by 5.0 % has been shown. Since the internal energy of the primary liquid is high, its heat content will also be high and thus the heat transfer from the primary to the secondary circuit will increase. So a similar effect like figures 5.1a through 5.2d can be observed.

Figures 5.4a through 5.4d represent the effect of reducing feed water flow rate by 5 % at the inlet of the secondary circuit. Since the flow rate is reduced in the secondary loop the amount of water receiving heat from the primary circuit is less. So the water in the secondary circuit will have higher

temperature and the quality will increase. Thus there will be an increase in pressure and flow rate. But the disturbance is very small, only 5.0 %. So these changes at the variables at the exit of the evaporator of the secondary circuit will also be very small.

Figures 5.5a through 5.5d indicate the effect of reducing pressure by 30.0 % at the inlet of the secondary circuit. The reduction in pressure will increase the quality and hence the mode of flow of the fluid in the secondary loop will be such that the heat transfer coefficient from the tube wall to the bulk of the fluid will increase which means an increased heat transfer rate. So the temperature will rise which in turn will affect the quality and this increase in quality will increase the pressure and mass flow rate.

Figures 5.6a through 5.6d indicate the effect of increasing the internal energy of the secondary liquid by 5.0 %. This increases the total heat content of the secondary fluid and hence the same phenomena as in figures 5.5a through 5.5d can be observed.

5.2 Conclusions:

In the present study it has been found that a 5.0 % change in the feed water flow rate at the entrance of the secondary circuit of the evaporator does not affect the function of the

steam generator very much. This trend was established by A.C. Pinto [7] in his attempt to find out how the steady state values at the exit of evaporator of the secondary circuit vary due to different feed water flow rates.

In all other cases the change in the variables at the outlet of the evaporator of the secondary circuit for some disturbances at the inlet conditions is large. This signifies that the mass flow rate, pressure and internal energy at the inlet of the primary circuit and the pressure and internal energy at the entrance of the secondary circuit play an important role in the operation of the steam generator.

If one examines the graphs carefully one will find that there are discontinuities in almost all the graphs at 0.4 sec. This may be due to numerical instability. The time step chosen for the present work is 0.001 sec. So further investigation can be made with reduced time step though this will take more of computer time.

Pressure at the exit of evaporator
of secondary circuit

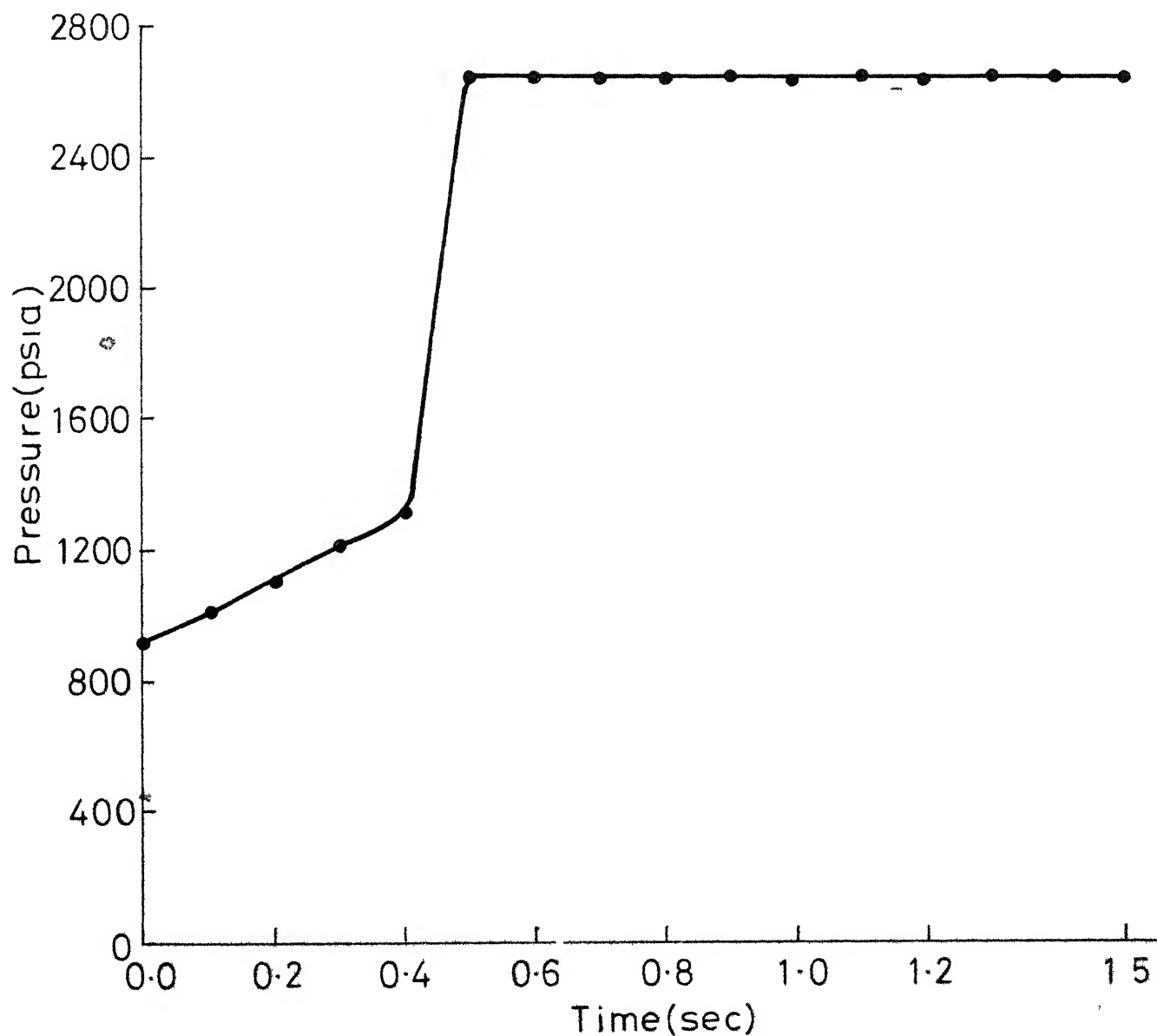


Fig. 5.1a Mass flow rate at the inlet of primary circuit was increased by 5.0%.

Temperature at the exit of evaporator
of the secondary circuit

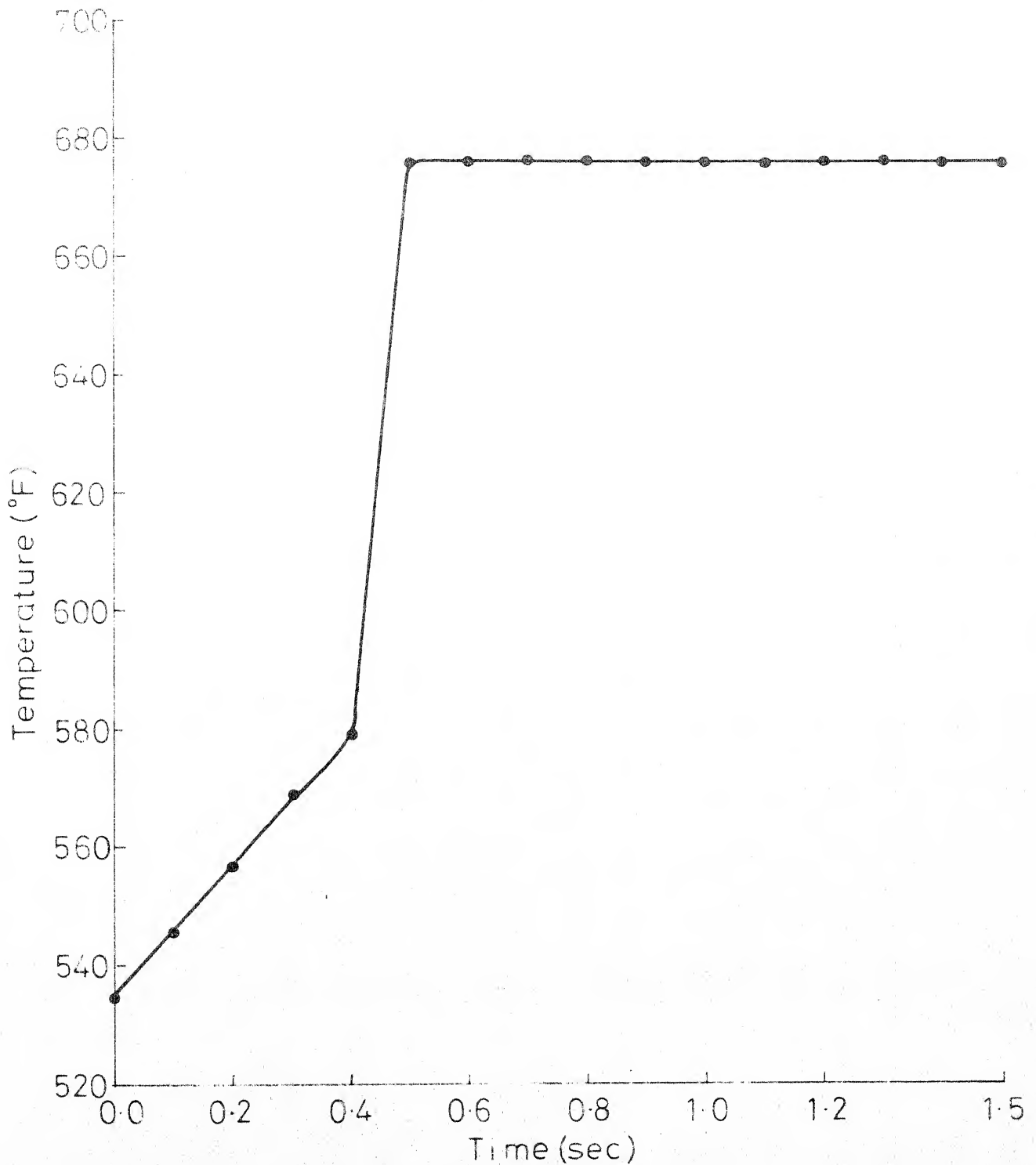


Fig. 5.1b Mass flow rate at the inlet of primary circuit was increased by 5.0%

Mass flow rate at the exit of evaporator
of the secondary circuit

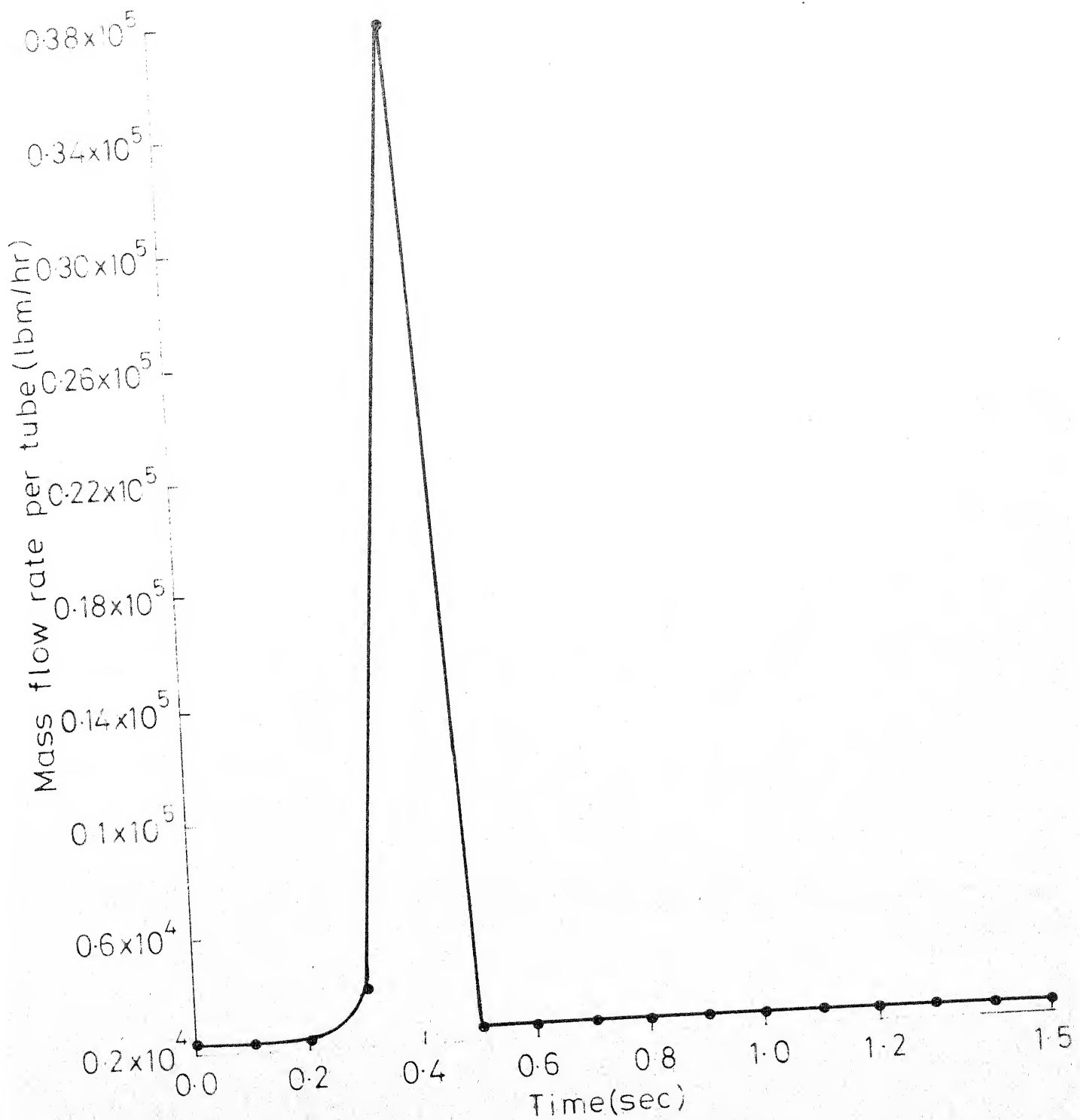


Fig. 5.1c Mass flow rate at the inlet of primary circuit was increased by 5.0%.

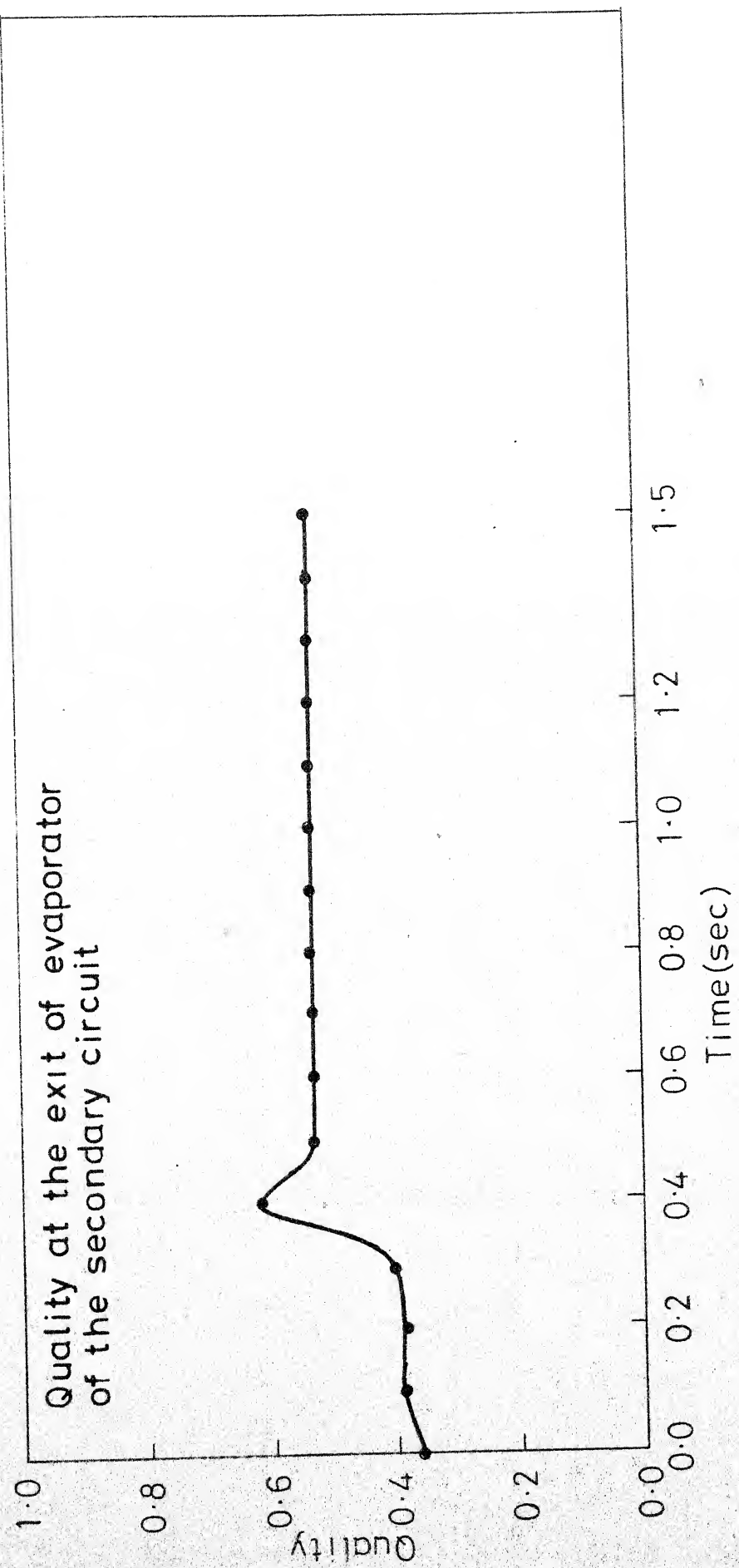


Fig. 5.1d Mass flow rate at the inlet of the primary circuit was increased by 5.0%

Pressure at the exit of evaporator of the secondary circuit

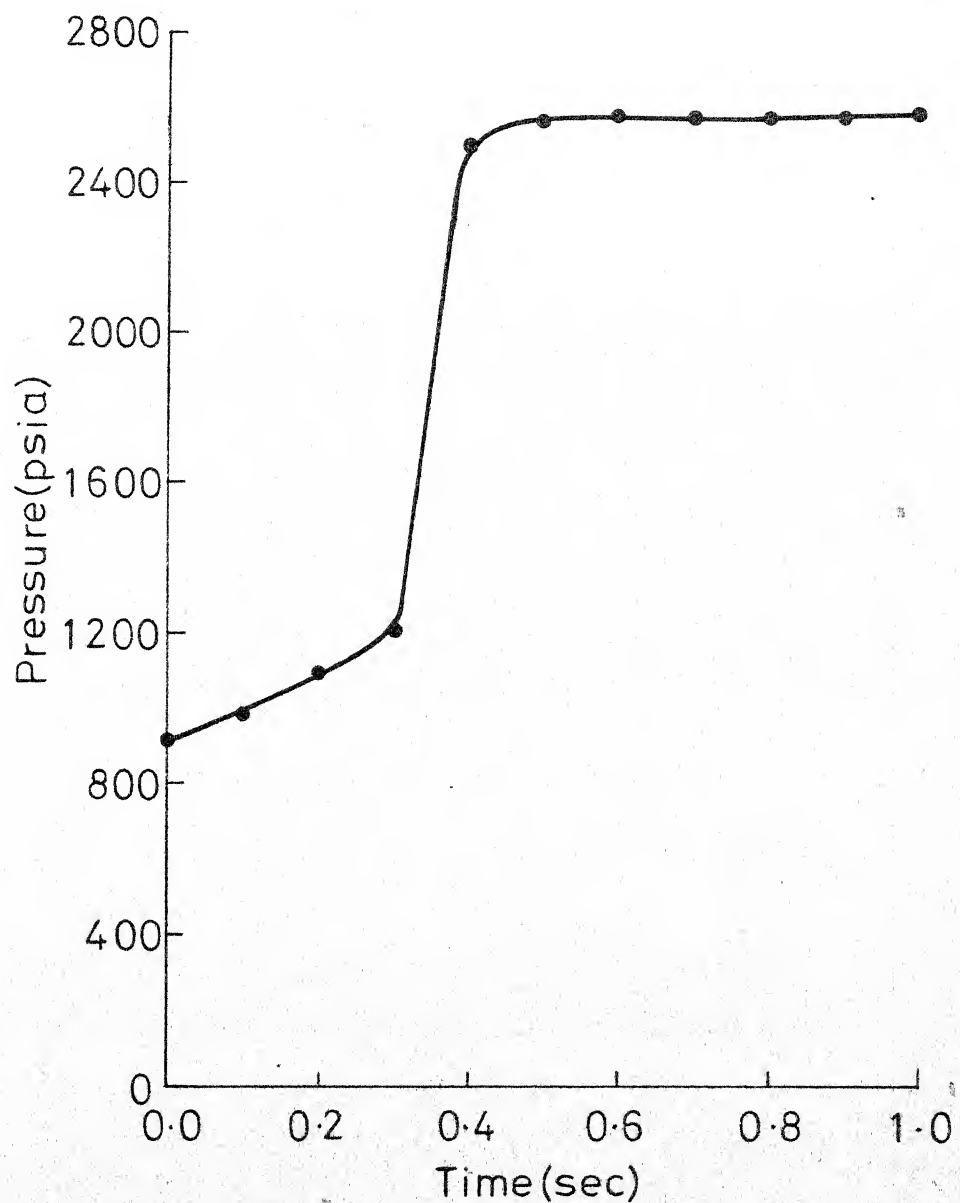


Fig. 5.2. The pressure was reduced by 30% at the entrance of evaporator of the primary circuit

Temperature at the exit of evaporator of the secondary circuit

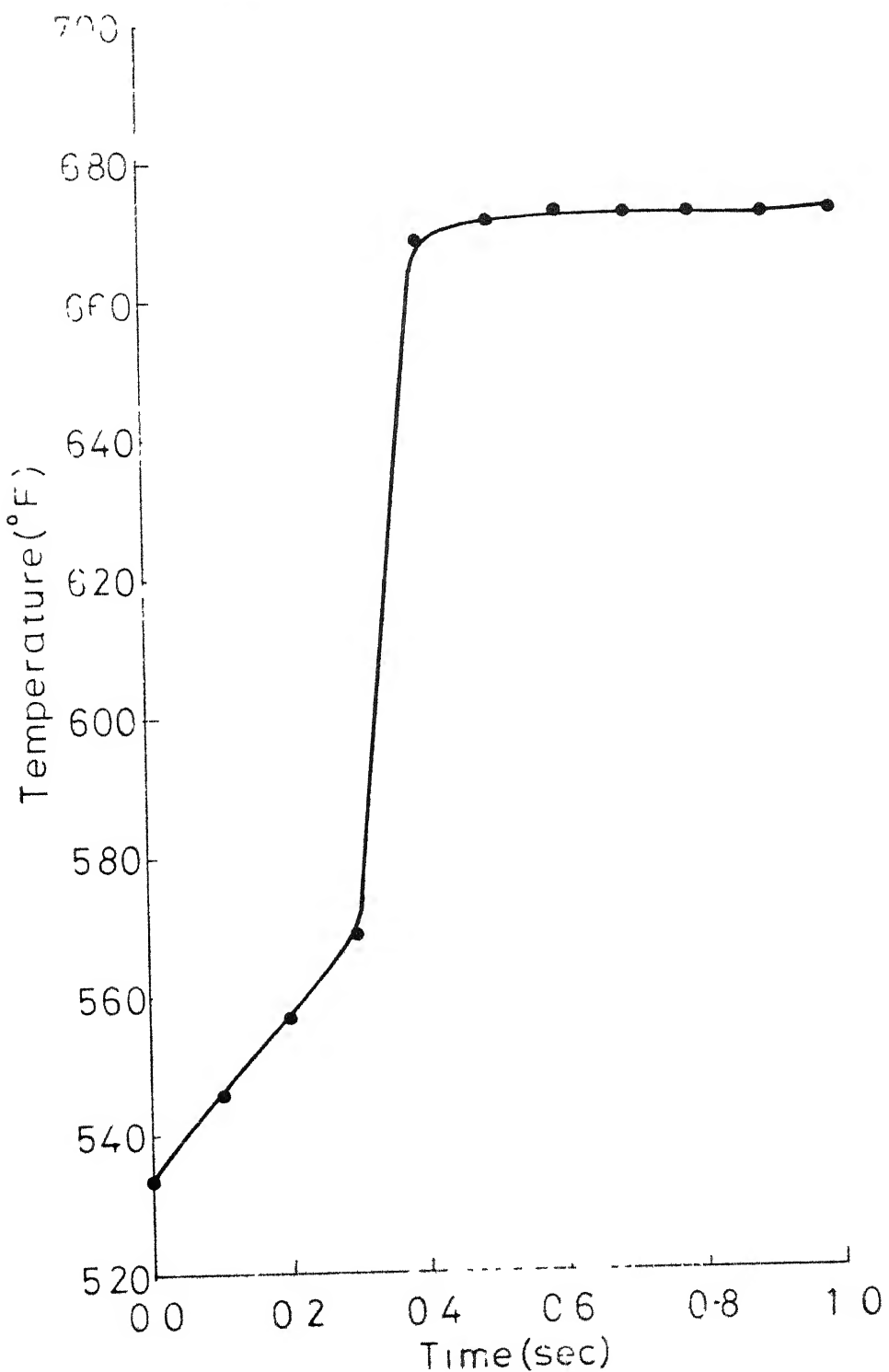


Fig 5.2b The pressure was reduced by 30% at the entrance of evaporator of the primary circuit

Mass flow rate at the exit of evaporator
of the secondary circuit

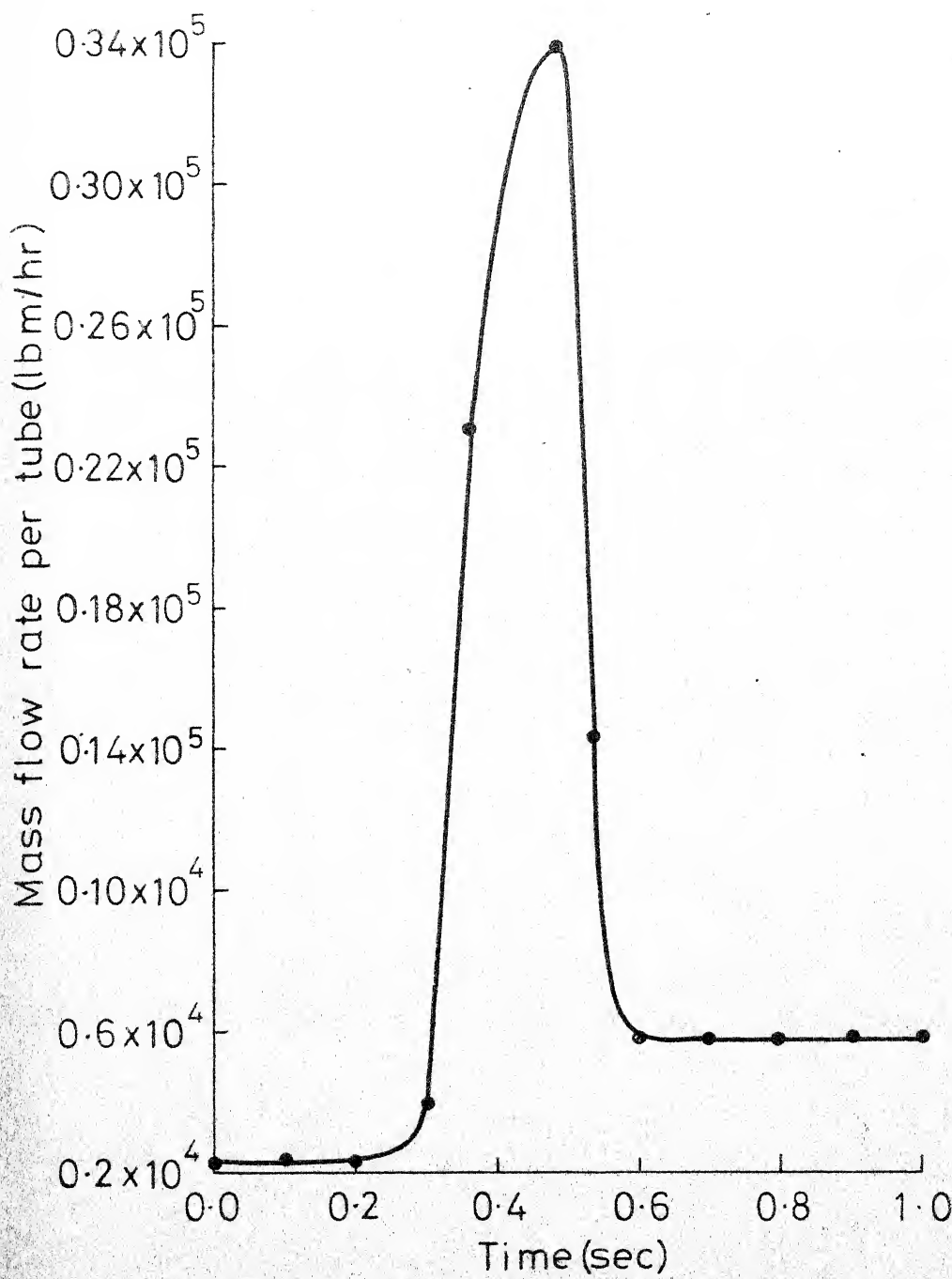


Fig. 5.2c The pressure at the inlet of evaporator of the primary circuit was reduced by 30.0%

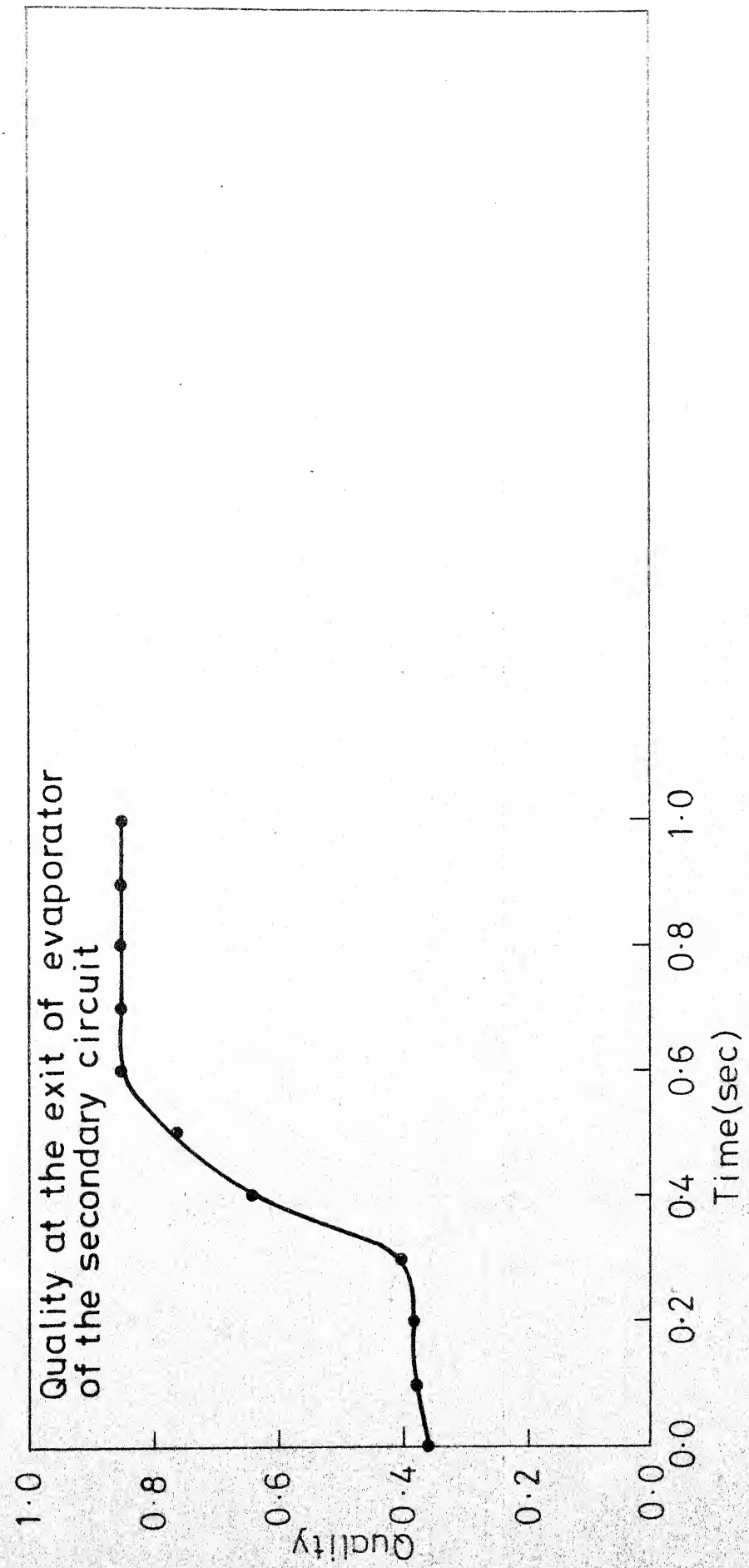


Fig. 5.2d Pressure was reduced by 30.0% at the inlet of evaporator of the primary circuit

Pressure at the exit of evaporator
of the secondary circuit

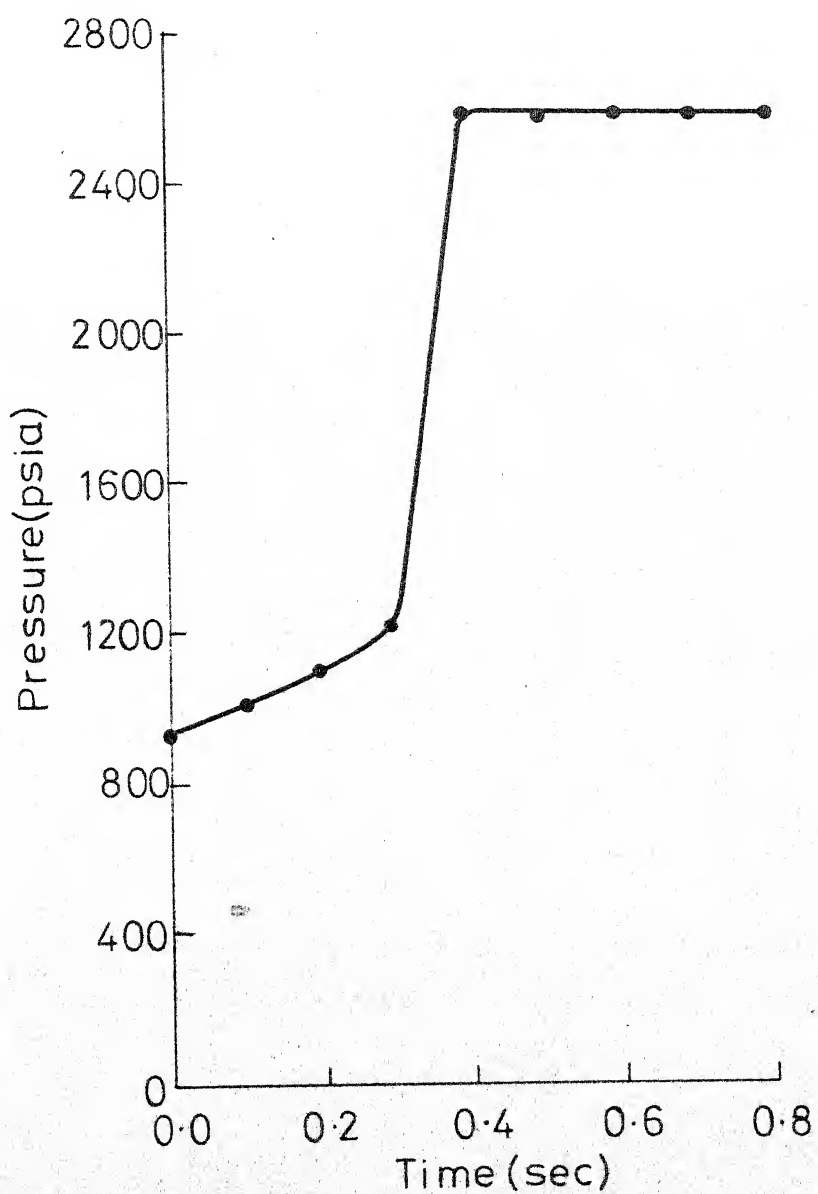


Fig. 5.3a The internal energy of the primary liquid was increased by 5.0% at the entrance of the evaporator

Temperature at the exit of evaporator
of the secondary circuit

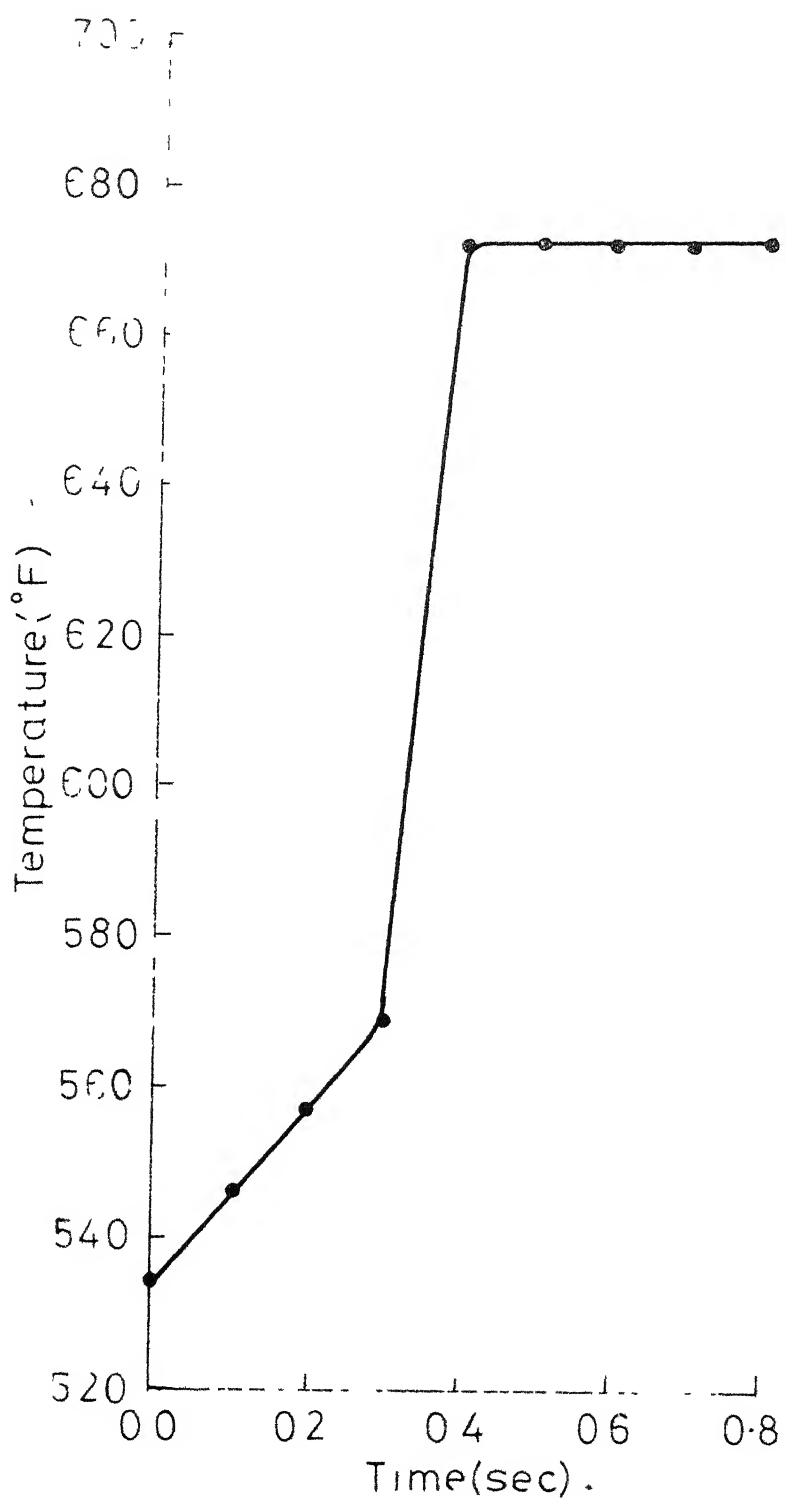


Fig. 5.3b The internal energy of the primary was increased by 5.0% at the inlet of the evaporator

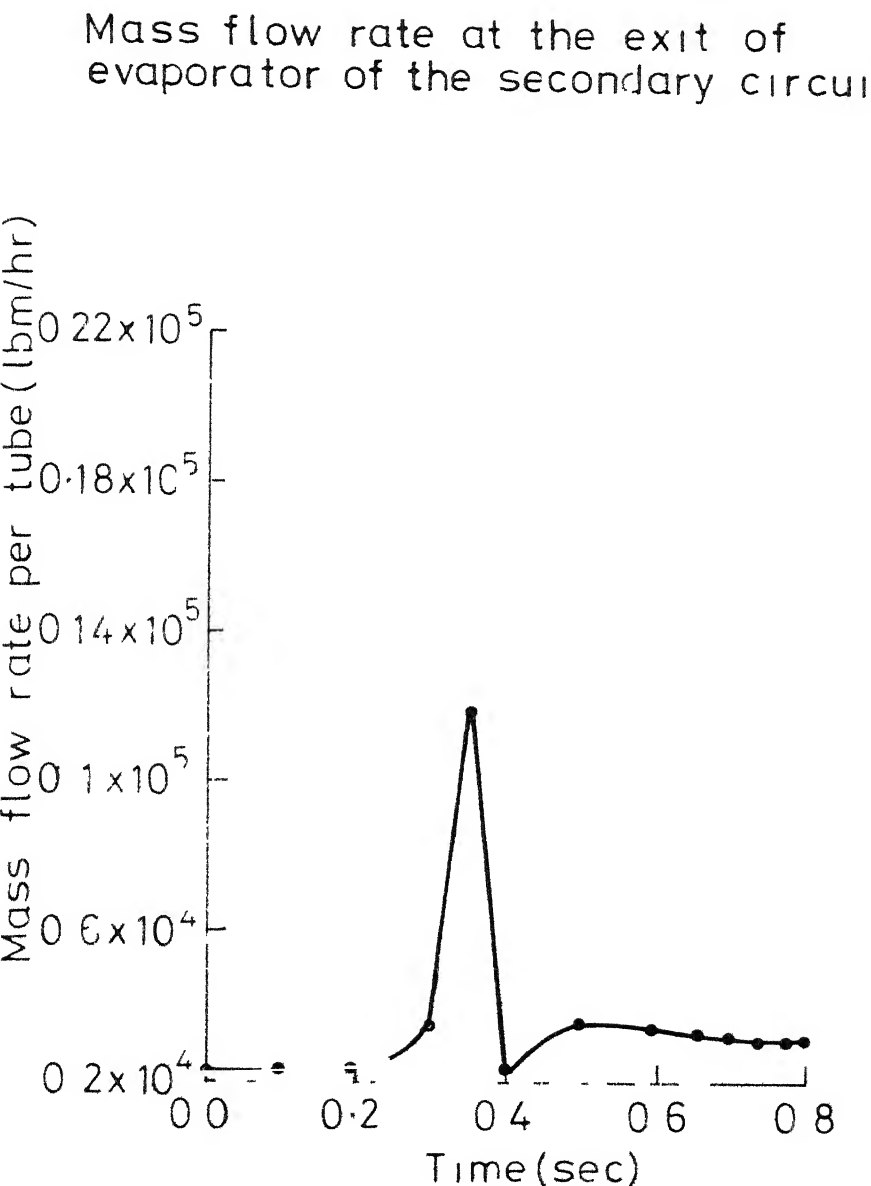


Fig. 5.3c The internal energy of primary liquid was increased by 5.0% at the entrance of the evaporator

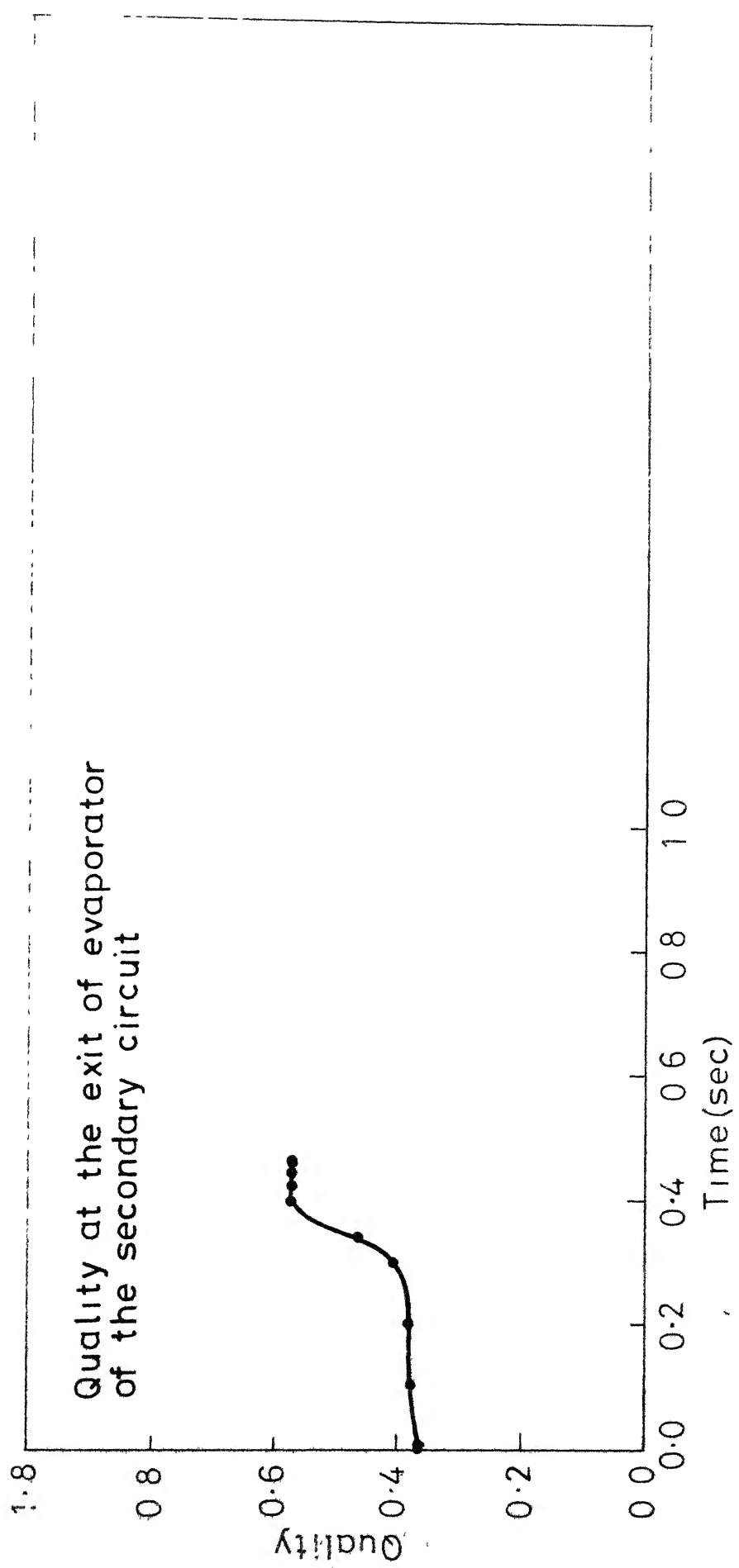


Fig. 5.3d The internal energy of primary liquid was increased by 5.0% at the entrance of the evaporator

Pressure at the exit of evaporator of the secondary circuit

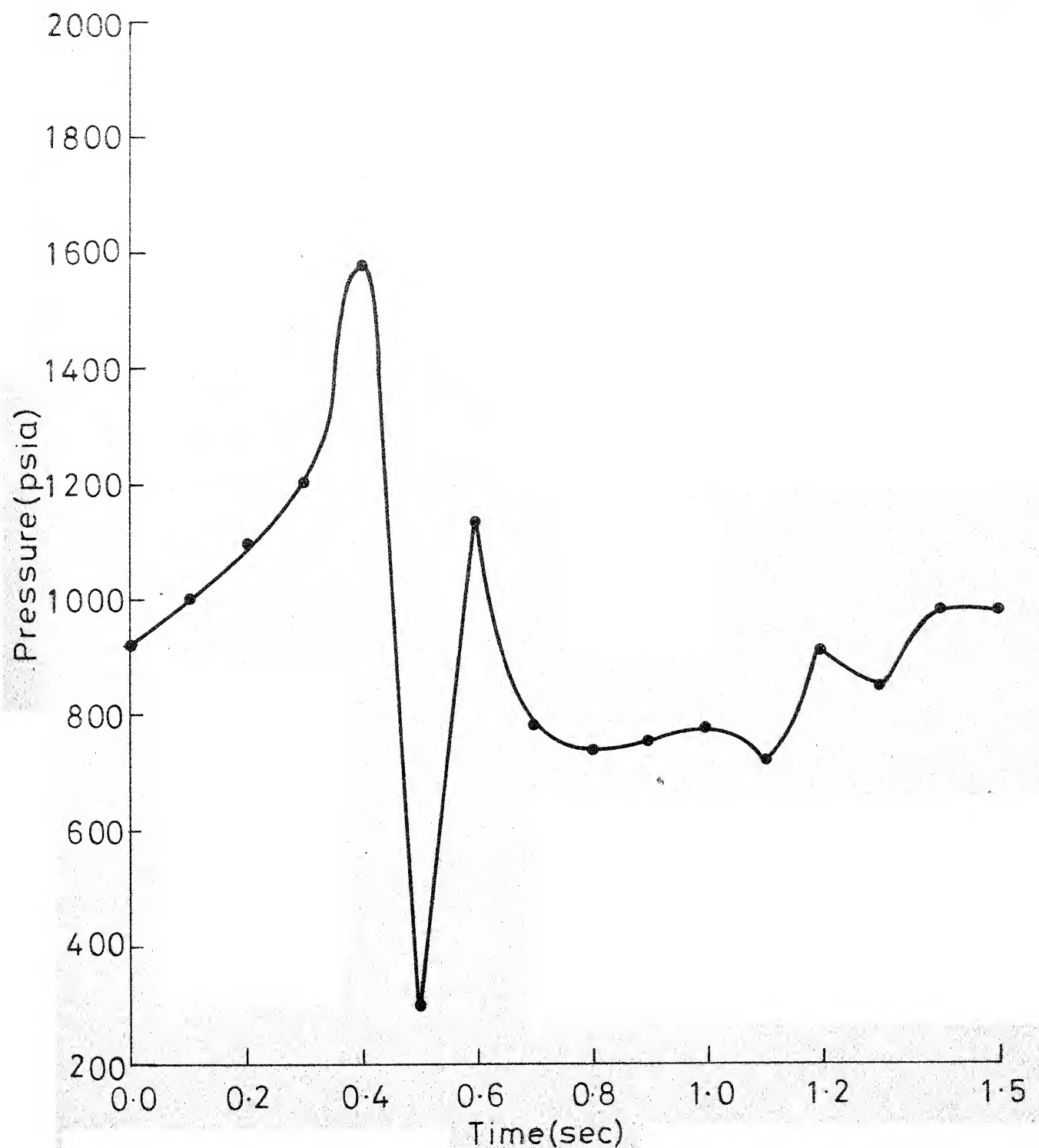


Fig. 5.4a Mass flow rate at the inlet of the secondary circuit was reduced by 5.0 %

Temperature at the exit of evaporator of the secondary circuit

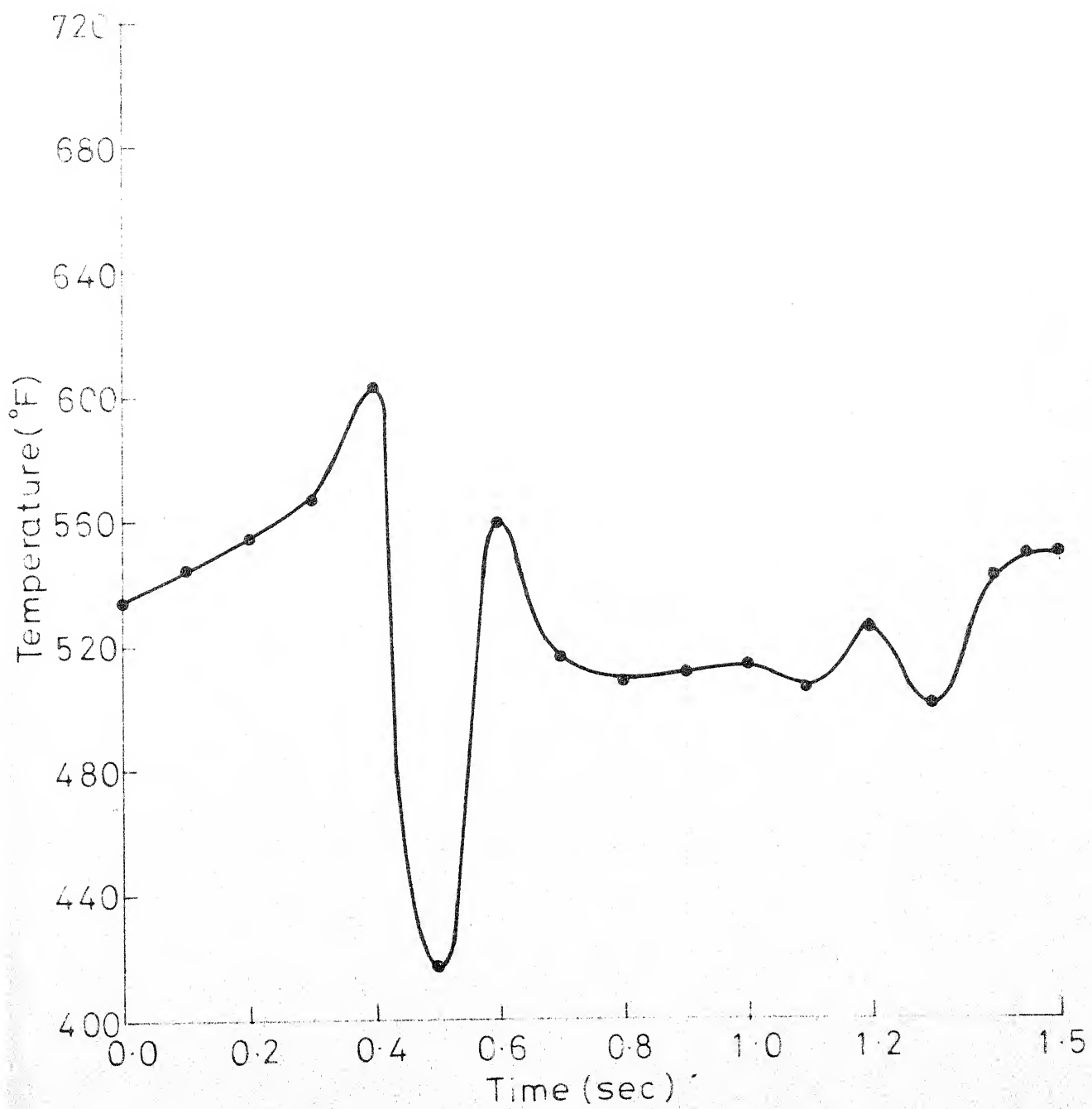


Fig. 5.4b Mass flow rate at the inlet of the secondary circuit was reduced by 5.0%

Mass flow rate at the exit of evaporator
of the secondary circuit

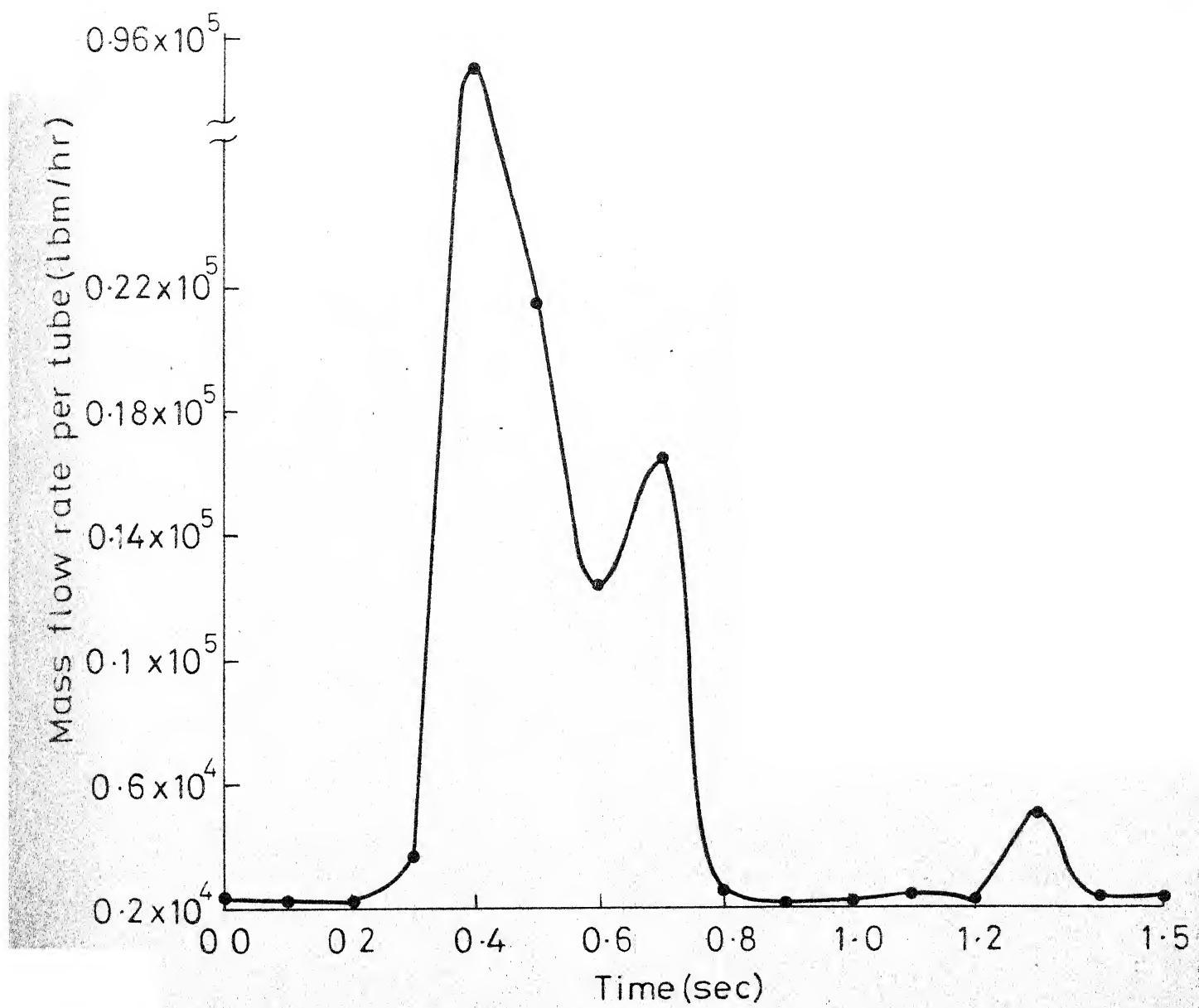


Fig. 5.4c Mass flow rate at the inlet of evaporator
of the secondary circuit was reduced
by 5.0%.

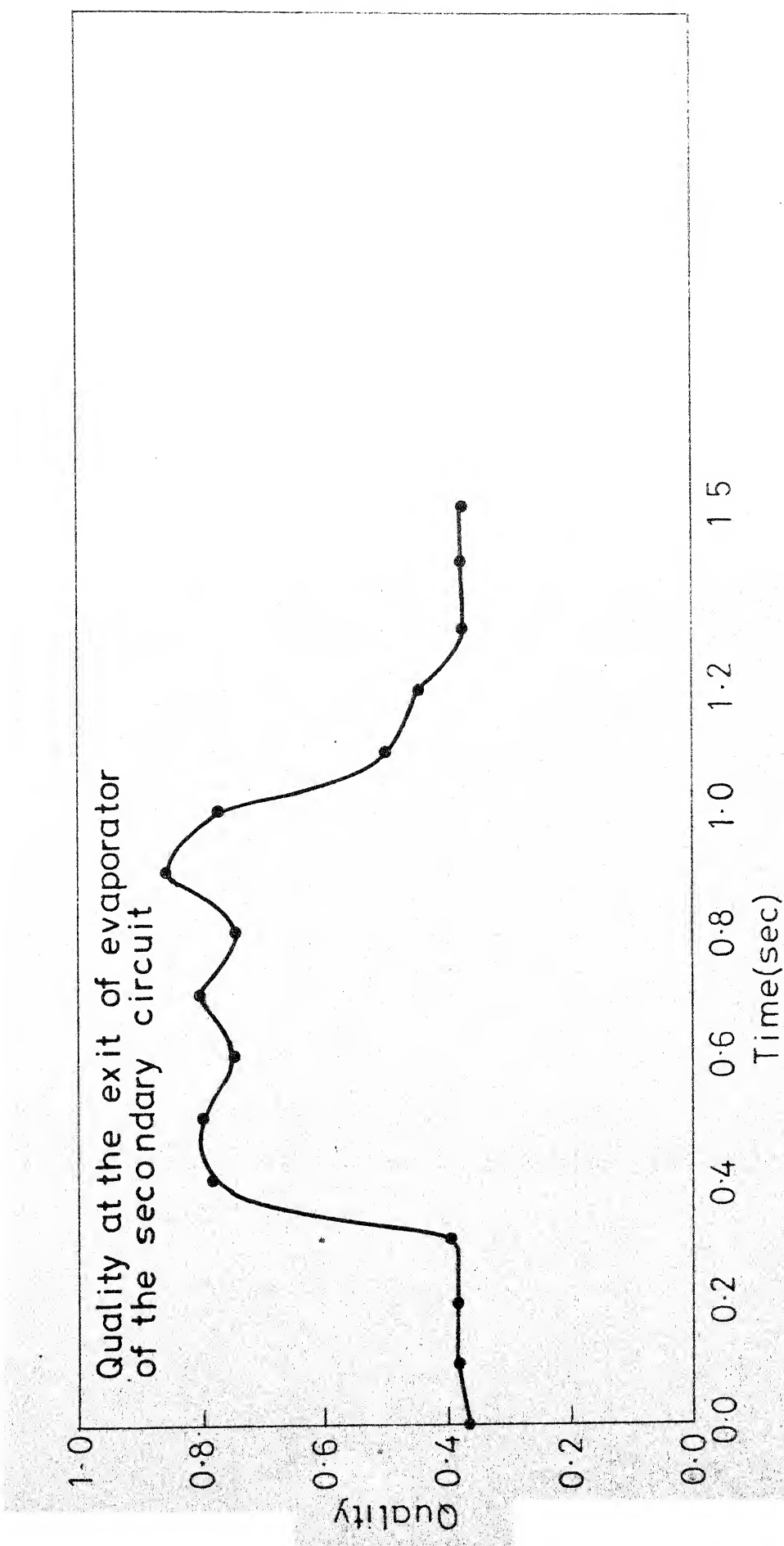


Fig. 5.4d Mass flow rate at the inlet of secondary circuit was reduced by 5.0%

Pressure at the exit of evaporator
of the secondary circuit

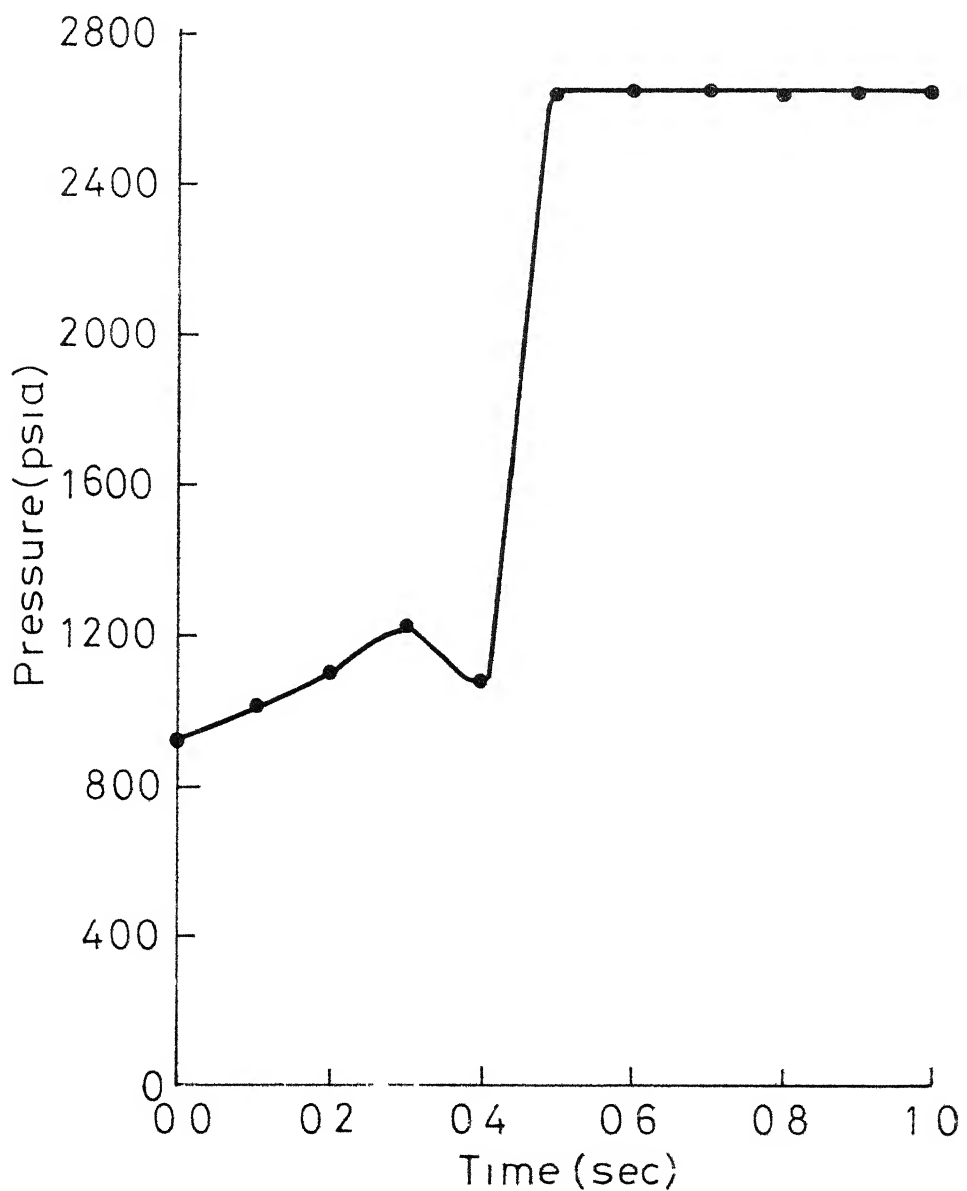


Fig. 5.5a The pressure at the inlet of the secondary circuit was reduced by 30.0%

Temperature at the exit of evaporator
of the secondary circuit

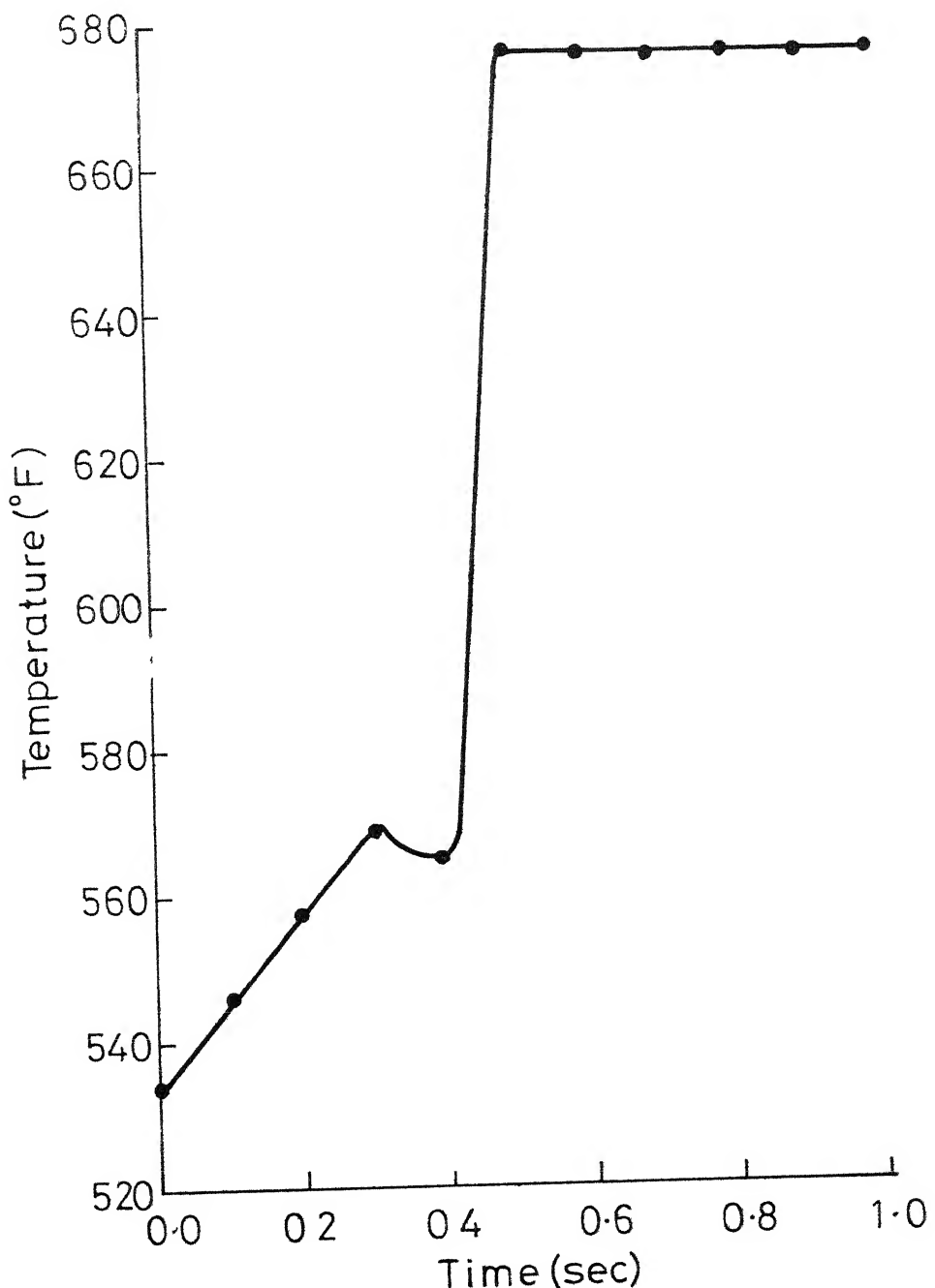


Fig. 5.5b The pressure at the inlet of the secondary circuit was reduced by 30.0%

Mass flow rate at the exit of evaporator
of the secondary circuit

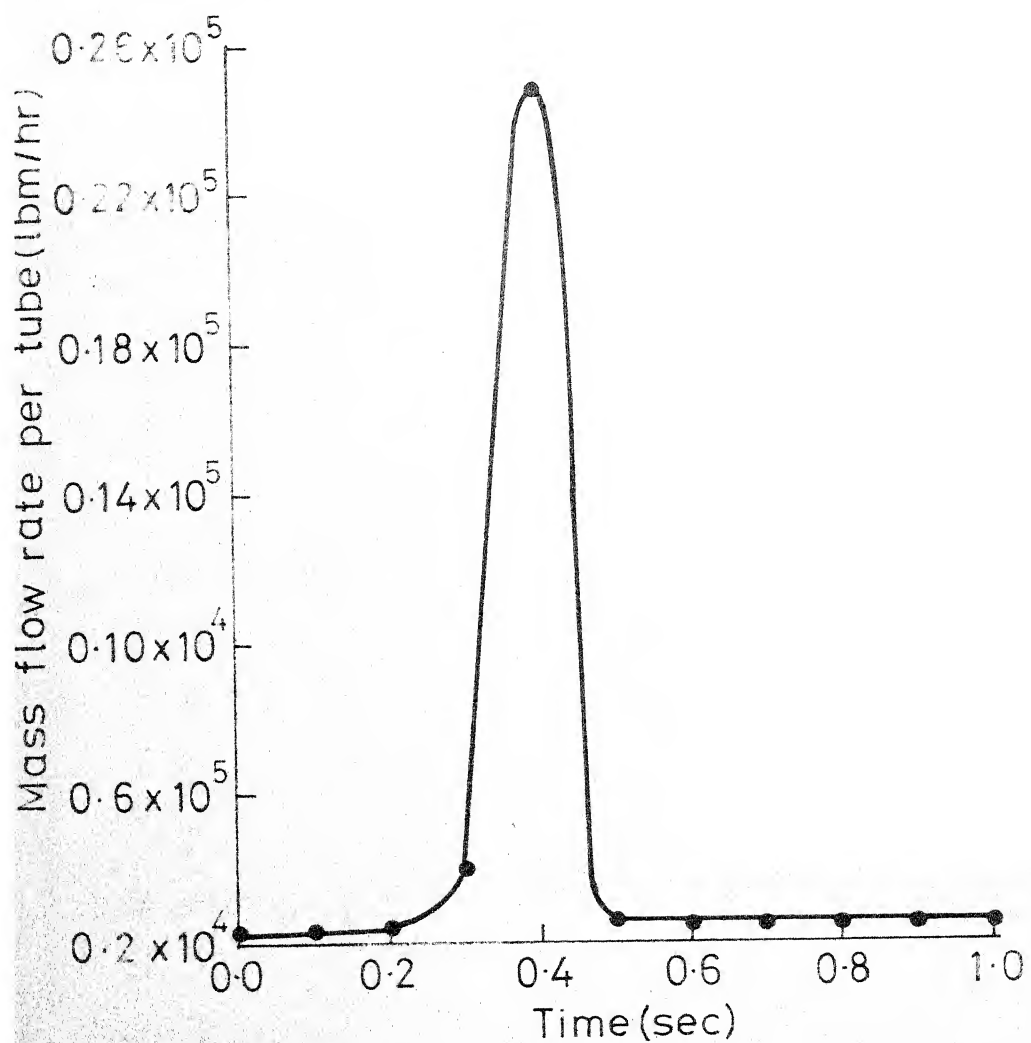


Fig. 5.5c The pressure at the inlet of the secondary circuit was reduced by 30.0%

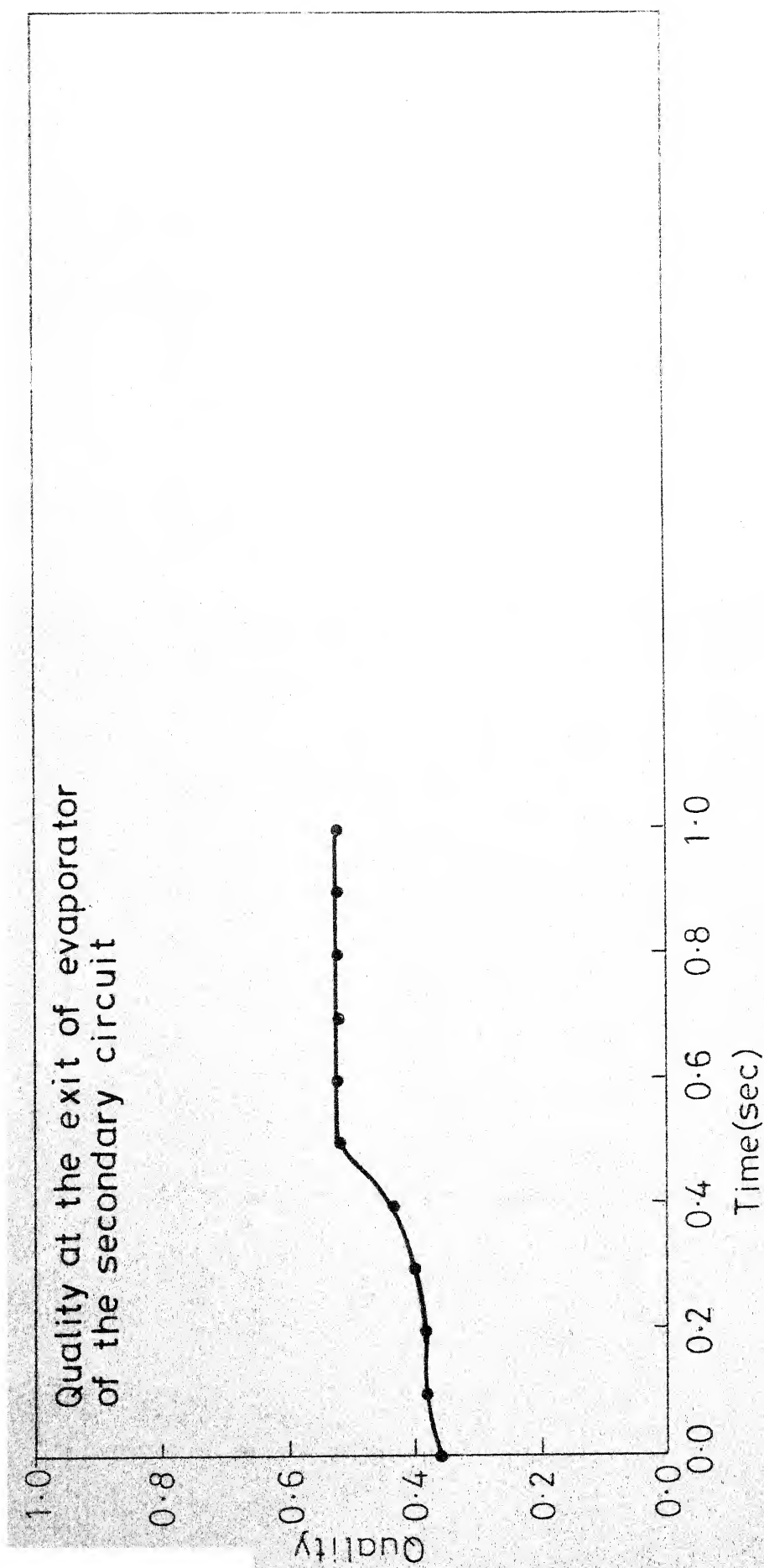


Fig. 5.5d The pressure at the inlet of the secondary circuit was reduced by 30.0%

Pressure at the exit of evaporator of the secondary circuit

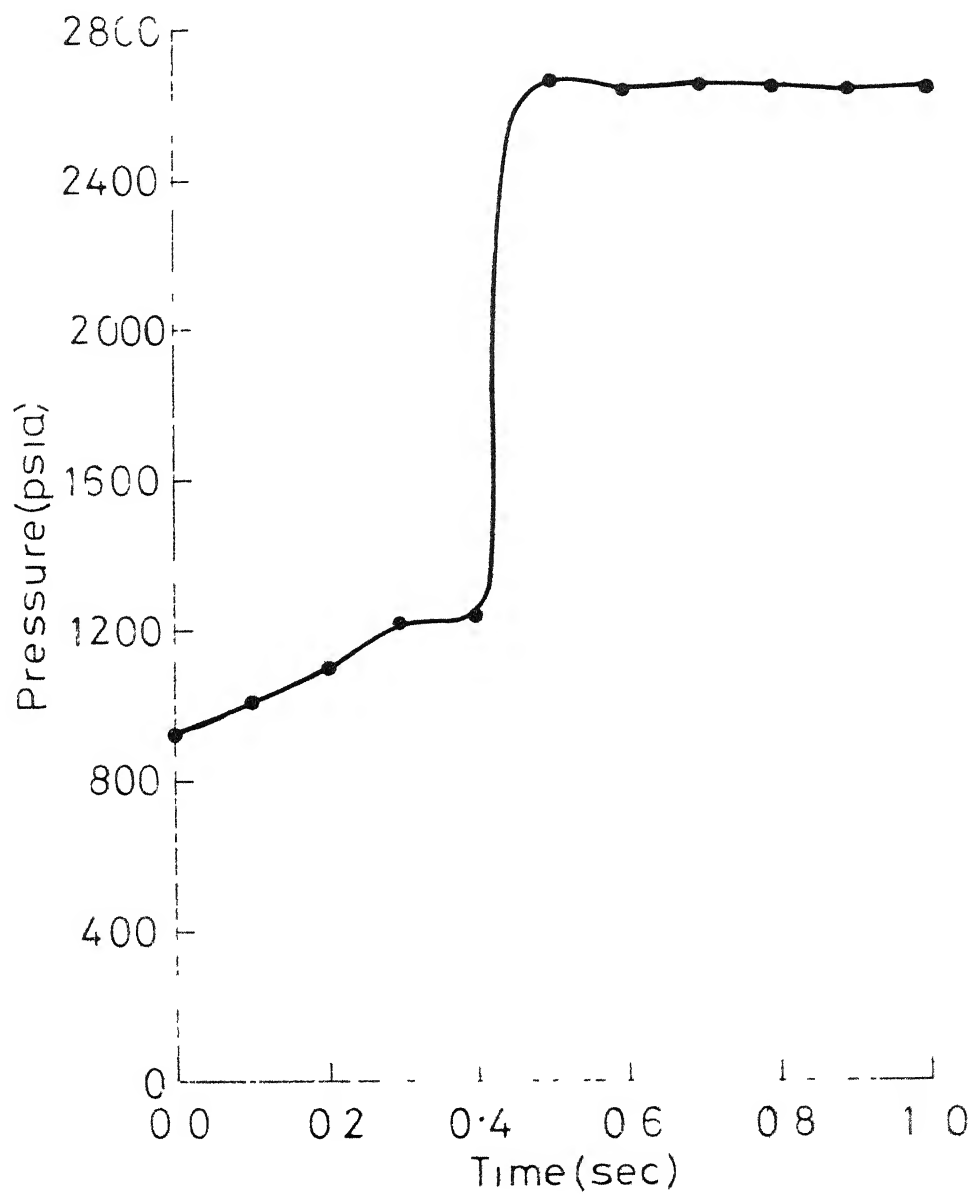


Fig. 5 6a The internal energy of secondary liquid was increased by 5%

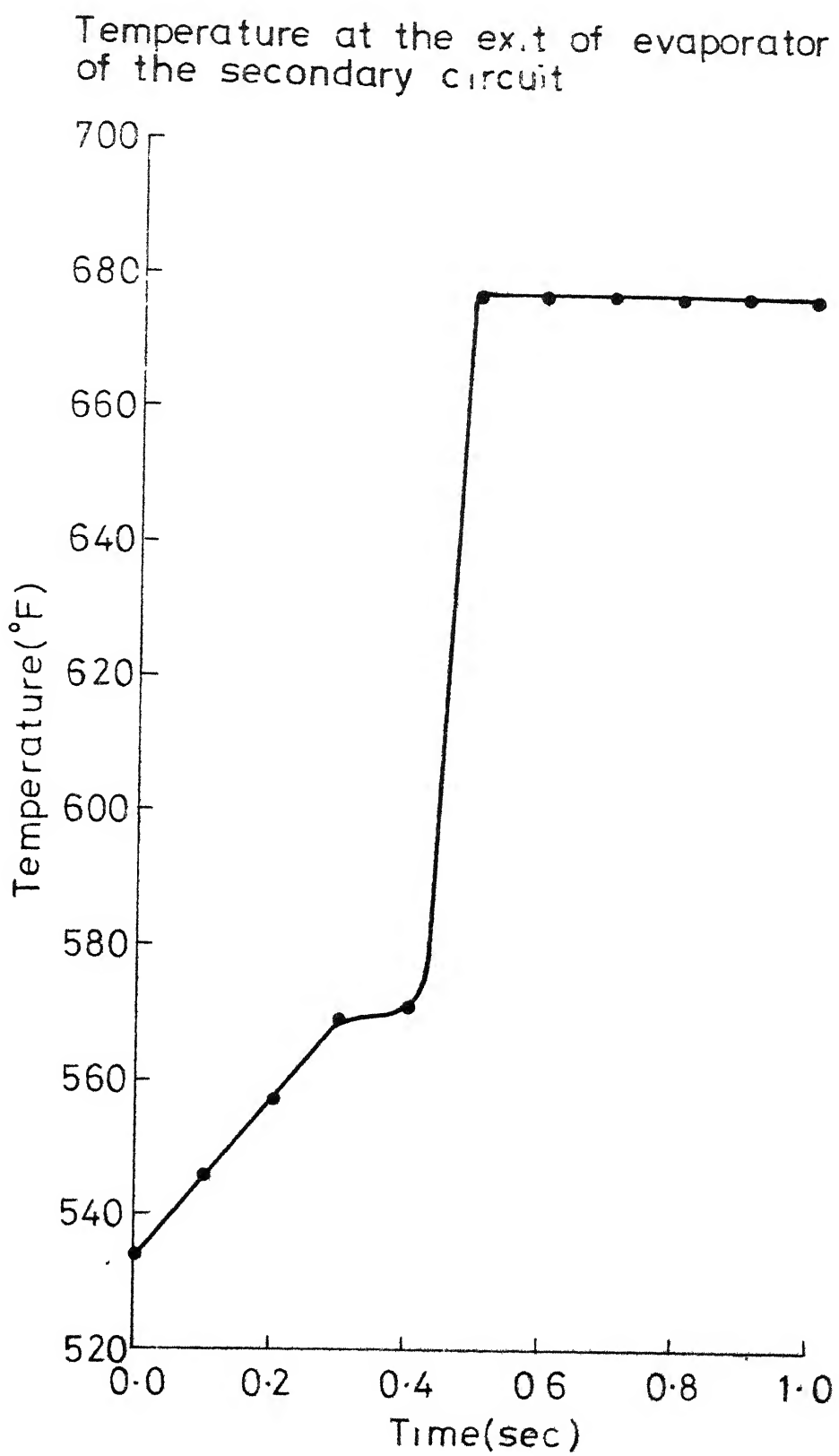


Fig. 5.6b The internal energy of secondary liquid was increased by 5.0 %

Mass flow rate at the exit of evaporator
of the secondary circuit

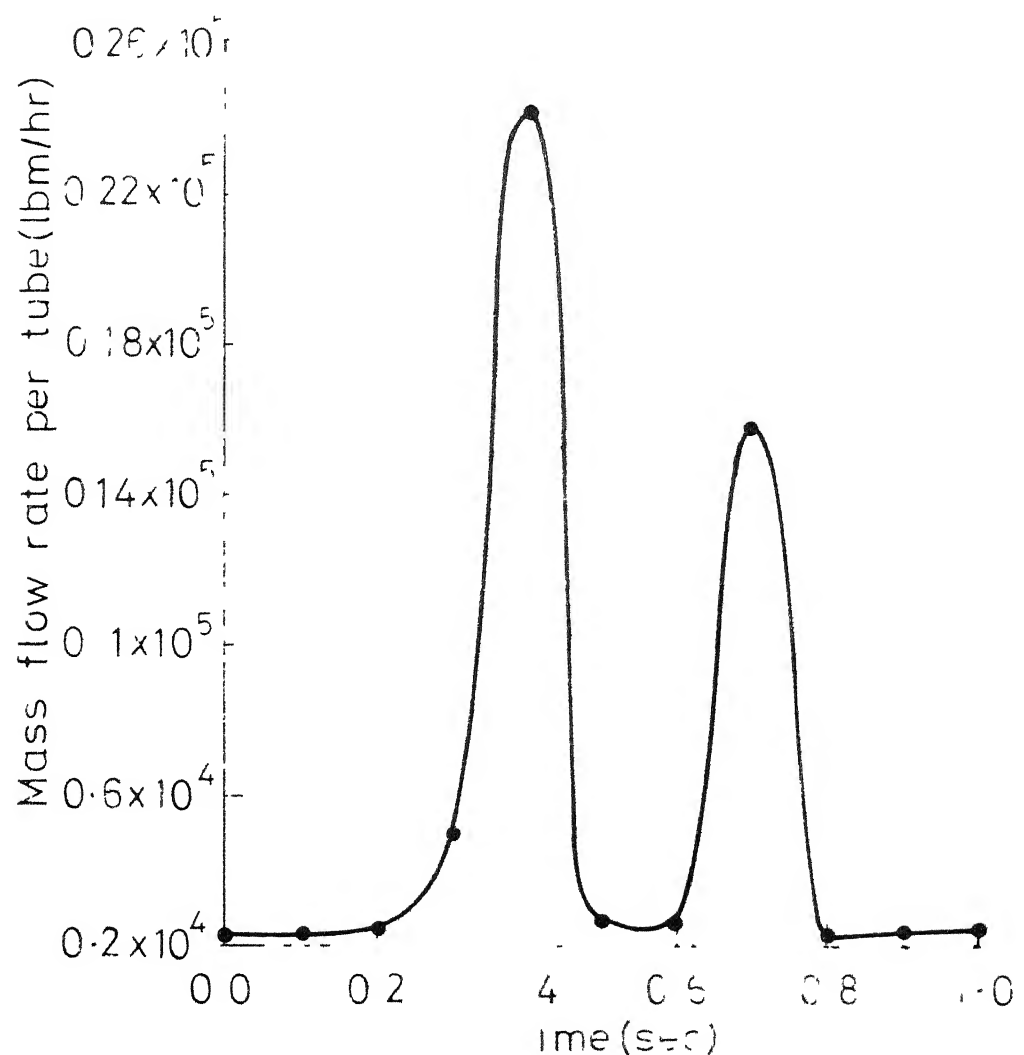


Fig. 5.6c The internal energy of secondary liquid was increased by 5.0%

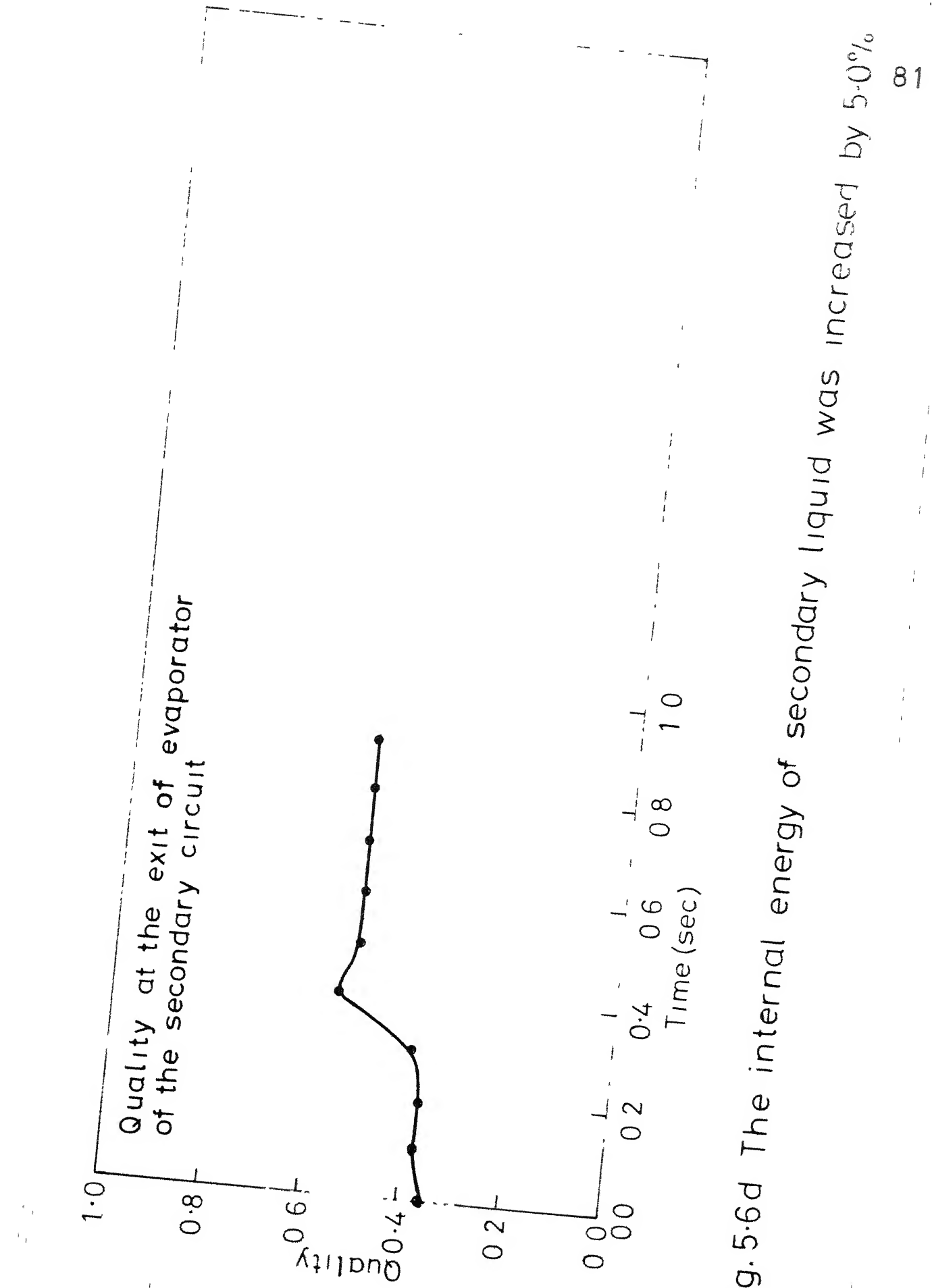


Fig. 5.6d The internal energy of secondary liquid was increased by 5.0%

APPENDIX A

We have

$$e = u + \frac{V^2}{2} + gZ$$

$$H = u + P/\rho$$

$$W = \rho AV$$

$$G = W/A$$

$$v = l/\rho$$

The last two terms of equation 3.5 can be written as

$$\begin{aligned} & \frac{d(We)}{dZ} + \frac{d}{dZ} (PAV) \\ &= \frac{d(We)}{dZ} + \frac{d}{dZ} \left(\frac{WP}{\rho} \right) \\ &= W \left\{ \frac{de}{dZ} + \frac{d}{dZ} \left(\frac{P}{\rho} \right) \right\} \end{aligned} \quad (a)$$

$$\text{Now } e = u + \frac{V^2}{2} + gZ = H - \frac{P}{\rho} + \frac{V^2}{2} + gZ$$

$$\therefore \frac{de}{dZ} = \frac{dH}{dZ} - \frac{d}{dZ} \left(\frac{P}{\rho} \right) + V \frac{dV}{dZ} + g$$

$$\text{i.e., } \frac{de}{dZ} + \frac{d}{dZ} \left(\frac{P}{\rho} \right) = \frac{dH}{dZ} + g + V \frac{dV}{dZ} \quad (b)$$

$$\text{But } V \frac{dV}{dZ} = \frac{W}{\rho A} \frac{d}{dZ} \left(\frac{W}{\rho A} \right) = \frac{1}{\rho} \left(\frac{W}{A} \right)^2 \frac{d}{dZ} \left(\frac{1}{\rho} \right)$$

$$= v G^2 \frac{dv}{dZ} \quad (c)$$

From equation (a), (b) and (c) we get,

$$\frac{d(\text{We})}{dz} + \frac{d}{dz} (\text{PAV}) = W \left(\frac{dH}{dz} + g + v G^2 \frac{dv}{dz} \right)$$

So equation 3.5 will become

$$\ddot{q} \frac{dA_T}{dz} - W \frac{dH}{dz} - W G^2 v \frac{dv}{dz} - Wg = 0$$

APPENDIX B

Equation 3.6 is

$$- A \frac{dP}{dz} - \frac{dF_K}{dz} - \frac{d(WV)}{dz} - A\rho g = 0$$

Now let us integrate this equation with respect to z from the centre of control volume $(n-1)$ to the centre of control volume n .

The first term will give

centre at
C.V.(n)

$$\int_{\text{centre of C.V.}(n-1)}^{\text{centre of C.V.}(n)} \frac{dP}{dz} dz = (P)_{\text{centre of C.V.}(n)} - (P)_{\text{centre of C.V.}(n-1)}$$

$$= \bar{P}_n - \bar{P}_{n-1}$$

where $\bar{P}_n = (P)_{\text{at the centre of C.V.}(n)}$

The second term will become

$$\int_{\text{centre of C.V.}(n-1)}^{\text{centre of C.V.}(n)} \frac{dF_K}{dz} dz = \int_{\text{centre of C.V.}(n-1)}^{\text{J.n.}} dF_K + \int_{\text{J.n.}}^{\text{centre of C.V.}(n)} dF_K$$

$$= \frac{1}{2} [\bar{F}_{K,n-1} + \bar{F}_{K,n}]$$

'J.n' represents junction n.

From the third term we get

$$\begin{aligned} & \text{centre of } C.V.(n) \quad \quad \quad J.n \quad \quad \quad \text{centre of } C.V.(n) \\ & \int \frac{d(WV)}{dz} dz = W \int dV + W \int dV \\ & \text{centre of } C.V.(n-1) \quad \quad \quad \text{centre of } C.V.(n-1) \quad \quad \quad J.n \\ & = W(V_{\text{at } J.n} - V_{\text{at the centre of } C.V.(n-1)}) \\ & \quad \quad \quad + W(V_{\text{at the centre of } C.V.(n)} - V_{\text{at } J.n}) \end{aligned}$$

The last term will become

$$\begin{aligned} & \text{centre of } C.V.(n) \\ & \int A \rho g dz = A \rho g \Delta Z = \frac{A g \Delta Z}{v} \\ & \text{centre of } C.V.(n-1) \end{aligned}$$

So if G is in lbm/ft²-hr and the pressure terms \bar{P}_n and \bar{P}_{n-1} are in psi, the equation 3.6 can be written as

$$\begin{aligned} \bar{P}_n = \bar{P}_{n-1} & - \frac{1}{2 \cdot A} (\bar{F}_{K,n-1} + \bar{F}_{K,n}) - \frac{G}{144 \cdot g_c} (V_n - \bar{V}_{n-1}) \\ & - \frac{G}{144 \cdot g_c} (\bar{V}_n - V_n) - \frac{g}{144 \cdot g_c} \cdot \frac{\Delta Z}{v_n} \end{aligned}$$

REFERENCES

1. RELAP4 - A computer code for transient thermal hydraulic Analysis, K.V. Moore and W.H. Rettig, USAEC Report, ANCR-1127 (1975).
2. FLASH - A computer code for PWR Thermal Hydraulic Analysis, J.A. Redfield and J.H. Murphy, Nucl. Appl. Technol, 6, 129 (1969).
3. D.G. Arwood and T.W. Kerlin, 'A Mathematical Model for an Integral Economizer U-Tube Steam Generator', Nuclear Technology, 35, 12 (1977).
4. A. Hoeld, 'A theoretical model for the calculation of large transients in nuclear natural-circulation U-tube steam generators (Digital code UTSG)', Nuclear Engineering and Design, 47, 1 (1978).
5. I.M.D. Silva, 'Codigo para simulacão de transients tipo PWR', Tese de Mestrado, Instituto Militar de Engenharia, Rio de Janeiro, Brasil, 1979.
6. Armando Costa Pinto and K. Sri Ram, 'Simulation of the PWR steam generator'. (To be published).
7. Armando Costa Pinto, 'Codigo para simulacão do gerador de vapor do reator nuclear PWR', Tese de Mestrado, Instituto Militar de Engenharia, Rio de Janeiro, Brasil, 1978.

8. L.S. Tong, Boiling Heat Transfer and Two-Phase Flow, John Wiley and Sons., Inc., N.Y., 1965.
9. L.S. Tong and J. Weisman, Thermal Analysis of Pressurized Water Reactors, American Nuclear Society, NY, 1970.
10. T.A. Porsching, J.H. Murphy and J.A. Redfield, Nucl. Sci. and Eng., 43, 218 (1971).
11. J.H. Keenan and F.G. Keyes, Thermodynamic properties of steam, John Wiley and Sons., Inc., NY, 1951.

REPORT OF TESTS

TEST 1 - TEST POINT 1 IS IN THE STEAM GENERATOR
WATER SIDE PRESSURE 0.5000E+12
WATER SIDE TEMP 0.32174E+02 BT/SEC**2
ACCUMULATOR 20 TO GENERATOR 0.32174E+02 BT/SEC**2
FRICTION PITCH

CHARACTERISTICS OF THE STEAM GENERATOR

NUMBER OF TUBES = 4671
PWT. OF TUBE 0.1500E+00 T.C.
INT. DIA. TUBE 0.6640E+00 T.C.
TOTAL HEAT TRANSFER AREA 0.48300E+05 FT**2
FURN. CAPAC. 0.00000E+00
SPEC. C. 0.10675E+01 T.C.
SECTIONAL PITCH

PRIMARY CIRCUIT

PRESSURE AT ENTRY 0.22500E+04 PSI
TEMP. AT ENTRY 0.62000E+03 DEGREE F
ENTHALPY AT ENTRY 0.64040E+03 BTU/LB
FLOW RATE 0.35550E+08 LB /HR
ESTIMATED STEAM PRESSURE 0.22300E+04 PSI
SECONDARY CIRCUIT

PRESSURE 0.11210E+04 PSI
TEMPERATURE 0.43000E+03 DEGREE F
ENTHALPY 0.40780E+03 BTU/LB
VAPOUR PRESSURE 0.92000E+03 PSI
QUALITY 0.10001E+00
VAPOUR FLOW RATE 0.40850E+07 LB/HR
RATE OF HEAT TRANSFER 0.32115E+10 BTU/HR

10110	3	1623303770	2	12409323144
10120	8	6	3	12409323144
10130	9	4	3	12409323144
10140	7	4	3	12409323144
10150	9	4	3	12409323144
10160	5	4	3	12409323144
10170	6	4	3	12409323144
10180	8	4	3	12409323144
10190	9	4	3	12409323144
10191	7	4	3	12409323144
10200	1	4	3	12409323144
10300	1	4	3	12409323144
10400	0	4	3	12409323144
10500	0	4	3	12409323144
10600	0	4	3	12409323144
10700	0	4	3	12409323144
10800	0	4	3	12409323144
10900	0	4	3	12409323144
11000	0	4	3	12409323144
11200	0	3	3	12409323144
11300	0	3	3	12409323144
11400	0	3	3	12409323144
11500	0	3	3	12409323144
11600	0	3	3	12409323144
11700	0	3	3	12409323144
11800	0	3	3	12409323144
11900	0	3	3	12409323144
12000	0	3	3	12409323144
12100	0	3	3	12409323144
12200	0	3	3	12409323144
12300	0	3	3	12409323144
12400	0	3	3	12409323144
12500	0	3	3	12409323144
12600	0	3	3	12409323144
12700	0	3	3	12409323144
12800	0	3	3	12409323144
12900	0	3	3	12409323144
13000	0	3	3	12409323144
13100	0	3	3	12409323144
13200	0	3	3	12409323144
13300	0	3	3	12409323144
13400	0	3	3	12409323144
13500	0	3	3	12409323144
13600	0	3	3	12409323144
13700	0	3	3	12409323144
13800	0	3	3	12409323144
13900	0	3	3	12409323144
14000	0	3	3	12409323144
14100	0	3	3	12409323144
14200	0	3	3	12409323144
14300	0	3	3	12409323144
14400	0	3	3	12409323144
14500	0	3	3	12409323144
14600	0	3	3	12409323144
14700	0	3	3	12409323144
14800	0	3	3	12409323144
14900	0	3	3	12409323144
15000	0	3	3	12409323144
15100	0	3	3	12409323144
15200	0	3	3	12409323144
15300	0	3	3	12409323144
15400	0	3	3	12409323144
15500	0	3	3	12409323144
15600	0	3	3	12409323144
15700	0	3	3	12409323144
16000	0	3	3	12409323144

0.01651	50.28	147.91	1138.1
0.01648	54.66	143.95	1136.9
0.01645	59.52	139.89	1134.4
0.01643	62.14	137.88	1132.7
0.01641	67.18	133.88	1130.9
0.01639	74.02	127.87	1129.3
0.01637	77.39	123.87	1128.3
0.01635	84.68	119.87	1126.6
0.01634	92.01	117.88	1125.7
0.01632	97.21	113.88	1124.1
0.01630	106.74	107.88	1122.4
0.01629	117.39	103.88	1121.0
0.01628	123.18	94.89	1119.2
0.01627	135.75	94.89	1118.4
0.01626	149.85	94.89	1117.7
0.01625	157.57	93.90	1115.7
0.01624	174.28	93.91	1114.7
0.01623	193.18	87.91	1113.2
0.01622	203.47	83.92	1111.6
0.01621	226.22	79.93	1109.8
0.01620	251.67	73.95	1107.2
0.01619	265.75	69.96	1105.2
0.01618	296.55	67.97	1104.4
0.01617	331.82	63.98	1102.7
0.01616	393.74	59.99	1100.9
0.01615	441.44	54.01	1098.4
0.01614	527.68	48.02	1096.6
0.01613	595.87	44.03	1095.8
0.01612	633.77	40.04	1094.1
0.01611	718.99	38.05	1092.3
0.01610	814.18	34.06	1091.5
0.01609	868.18	30.06	1088.0
0.01608	989.67	28.07	1087.2
0.01607	1129.77	24.07	1085.5
0.01606	1208.15	20.07	1083.7
0.01605	1383.55	18.07	1082.9
0.01604	1588.44	10.06	1079.4
0.01603	1704.99	8.05	1078.6
0.01602	2271.88	6.04	1077.7
0.01602	2271.88	4.03	1076.9
0.01602	2445.11	2.01	1076.9
0.01602	2632.22	0.01	1075.1
0.01602	2836.64		
0.01602	3060.47		
0.01602	3305.77		
0.001	0.003	4.68	6.70
0.000	0.003	3747	4881
0.000	0.003	8961	1104
0.000	0.003	10506	56072
0.000	0.003	117	167930
0.000	0.003	17	105280
0.000	0.003	19146	24845
0.000	0.003	1.0	1.0
0.000	0.003	247544F+01	23912
0.000	0.003	884860E+00	73168
0.000	0.003	409955F-01	0.00000
0.000	0.003	253467E+01	26337
0.000	0.003	783596E+00	89883
0.000	0.003	449483E-01	12451
0.000	0.003	948287E+00	60137
0.000	0.003	939490E-01	22198
0.000	0.003	386182E-01	13888
0.000	0.003	211601E+01	20987
0.000	0.003	574207E+00	14319
0.000	0.003	547085E-01	70141
0.000	0.003	383516E+00	62853

→ 63023

A. 63023

Date Slip

This book is to be returned on the date last stamped.

D 6.72.9

NETP-1980-M-KAR - DIG